REPUBLIC OF TÜRKİYE

ALTINBAŞ UNIVERSITY

Institute of Graduate Studies

Electrical and Computer Engineering

MACHINE LEARNING TECHNIQUES FOR ESTIMATION OF HUMAN TIREDNESS LEVEL FROM BRAIN ELECTRICAL ACTIVITY

Saad SHABAN

Doctor of Philosophy

Supervisor

Prof. Dr. Osman UÇAN

Istanbul, 2023

MACHINE LEARNING TECHNIQUES FOR ESTIMATION OF HUMAN TIREDNESS LEVEL FROM BRAIN ELECTRICAL ACTIVITY

Saad SHABAN

Electrical and Computer Engineering

Doctor of Philosophy

ALTINBAŞ UNIVERSITY

2023

The dissertation titled MACHINE LEARNING TECHNIQUES FOR ESTIMATION OF HUMAN TIREDNESS LEVEL FROM BRAIN ELECTRICAL ACTIVITY prepared by SAAD ABDULAZEEZ SHABAN and submitted on 5/4/2023 has been **accepted unanimously** for the degree of PhD in Electrical and Computer Engineering.

____
Prof. Dr. Osman Nuri UÇAN
Supervisor

Thesis Defence Committee Members:

Prof. Dr. Osman Nuri UÇAN	Department of Electrical Electronics Engineering, Altınbaş University	___________________
Assoc. Prof. Dr. Adil Deniz DURU	Department of Trainer Education, Marmara University	___________________
Asst. Prof. Dr. Sefer KURNAZ	Department of Computer Engineering, Altınbaş University	___________________
Asst. Prof. Dr. Abdullahi Abdu IBRAHIM	Department of Computer Engineering, Altınbaş University	___________________
Asst. Prof. Dr. Serdar KARGIN	Department of Biomedical Engineering, Arel University	___________________

I hereby declare that this dissertation meets all format and submission requirements of a PhD thesis.

Submission date of the thesis to Institute of Graduate Studies: ___/___/___

I hereby declare that all information/data presented in this graduation project has been obtained in full accordance with academic rules and ethical conduct. I also declare all unoriginal materials and conclusions have been cited in the text and all references mentioned in the Reference List have been cited in the text, and vice versa as required by the abovementioned rules and conduct.

Saad Abdulazeez SHABAN

Signature

DEDICATION

To my wonderful family, wife, and children

ACKNOWLEDGEMENTS

My biggest gratitude goes to my lord ALLAH for the mercy and success he gave me, to his beloved prophet MOHAMMED peace be upon him. Great thanks to my academic supervisor, Prof. Dr. Osman Nuri UÇAN and co-supervisor, Assoc. Prof. Dr Adil Deniz DURU for their continuous support, advice, and encouragement during my work. Special thanks are extended to the soul of my father who had been the man that brought me up to walk through this path, to my lovely mother who hadn’t forget me by her preys, to my wonderful wife for her continuous support and patience during the hard times of my academic study. Also, to my sons and daughter, who have been my biggest source of strength in my way. Special thanks to my friend Usama Al-Samarai for his assistance. I’d tell them all that they represent important achievements in my life. From the bottom of my feelings, I’d like to thank all my loving brothers and sisters, natives, friends, and teachers, without whom, I wouldn’t be in this position.

ABSTRACT

MACHINE LEARNING TECHNIQUES FOR ESTIMATION OF HUMAN TIREDNESS LEVEL FROM BRAIN ELECTRICAL ACTIVITY

SHABAN, Saad

PhD, Electrical and Computer Engineering, Altınbaş University,

Supervisor: Prof. Dr. Osman Nuri UÇAN

Co-Supervisor: Assoc. Prof. Adil Deniz DURU

Date: April/2023

Pages: 86

Electroencephalography (EEG) signals have been used in the recent years to investigate various brain activities for different scopes, like the important field of neuroscience. While a good number of studies concerned to the sports filed, minority of them were dedicated to study the changes encountered to the body vital signs happening after performing acute exercise. One of the important body signs is the fatigue state that derives the increase of lactate enzyme in the blood. It was employed by our study as a fatigue sign that may be predicted to see if it can discriminate between different enzyme levels. Signal pre-processing techniques were applied to the raw EEG signals, as they are highly contaminated with noises and artefacts, to clean them and get noise-free data. Our work offers a system scheme that extracts two features and passes them to classifiers to discriminate between lactate levels reflecting body tiredness levels. Firstly, the linear Band Power (BP), and secondly the proximity measure of Sample Entropy (SaEn) of EEG signals used. Variety of classification models accepts data from the previous stage to classify them. Classification task happened in 2 steps, in the first only 2 classes, low-tired and high-tired were discussed, whereas the second step discussed 3 classes, low-tired, moderate-tired, and high-tired, that reflects different lactate enzyme levels low, mid, or high. Data collected by a specialised acquisition device from 16 brain electrodes from a group of elite class athletes in a resting state condition. Two sessions of data recordings were studied, before and after performing acute aerobic exercise bout. Classification results were validated against blood lactate measurements taken before and after the exercise. Findings were presented in the Results chapter of this reveal that our system achieved high prediction scores and provides a promising tool to investigate levels of lactate enzyme non-invasively, which is novel and hadn’t been studied before for the best of our knowledge. Findings may be employed in fields like Brain-Computer Interface (BCI), applications of Internet of Things (IoT), biomedicine and other fields, off-line or on-line especially when true prediction rate is crucial and affect the application efficiency.

Keywords: Electroencephalography, Feature Extraction, Classification, Band Power, Sample Entropy.

TABLE OF CONTENTS

Pages

LIST OF TABLES

Pages

LIST OF FIGURES

Pages

ABBREVIATIONS

EEG	:	Electroencephalogram
BP	:	Band Power
SaEn	:	Sample Entropy
BCI	:	Brain Computer Interface
IoT	:	Internet of Things
MRI	:	Magnetic Resonance Imaging
BOLD	:	Blood Oxygenated Level Dependency
FFT	:	Fast Fourier Transform
DFT	:	Discrete Fourier Transform
PTCS	:	Physical Tiredness Classification System
ADHD	:	Attention Deficit Hyperactivity Disorder
SVM	:	Support Vector Machine
LDA	:	Linear Discriminant Analysis
DT	:	Decision Tree
LR	:	Logistic Regression
K-NN	:	K-Nearest Neighbour
SSE	:	Steady State Exercise
EE	:	Exhaustive Exercise
ECG	:	Electrocardiogram
DDE	:	Delay Differential Equations

iAPF	:	individual Alpha Peak Frequency
SCCT	:	Sport Concussion Assessment Tool
K-D test	:	King-Devick test
SWI	:	Small World Index
WPLI	:	Weighted Phase Lag Index
BLa	:	Blood Lactate Levels
DBD	:	Descriptive Behaviour Disorder
sLORETA	:	standardised Low Resolution Brain Electromagnetic Tomography
MVC	:	Maximum Voluntary Contraction
ANN	:	Artificial Neural Network
ICC	:	Intraclass Correlation Coefficient
CoV	:	Coefficient of Variation
MEMD	:	Multivariate Empirical Mode Decomposition
HEOG	:	Horizontal Electrooculography
VEOG	:	Vertical Electrooculography
SSS	:	Sensation Seeking Scale
fMRI	:	functional Magnetic Resonance Imaging
fNIRS	:	functional Near-Infrared Spectroscopy
MEG	:	Magnetoencephalography
LORETA	:	Low Resolution Brain Electromagnetic Tomography
AE	:	Approximation Entropy

DE	:	Differential Entropy
PE	:	Permutation Entropy
FE	:	Fuzzy Entropy
MSE	:	Multi Scale Entropy
IMF	:	Intrinsic Mode Functions
RPE	:	Rated Perceived Exertion
TP	:	True Positive
TN	:	True Negative
FP	:	False Positive
FN	:	False Negative
ROC	:	Receiver Operator Characteristics
AUC	:	Area Under Curve
PSD	:	Power Spectral Density
NAD	:	Nicotinamide Adenine Dinucleotide
ATP	:	Adenosine Triphosphate
CoA	:	acetyl-Coenzyme A
GADP	:	Glyceraldehyde 3-Phosphate
1,3BPG	:	1,3-Bisphosphoglycerate
LDH	:	Lactate Dehydrogenase

LIST OF SYMBOLS

π	:	Circumference Ratio
ρ	:	SVM Hyperplane
x_r	:	Point x Extension on ρ
α	:	Rescale Factor

1. INTRODUCTION

Electroencephalography represents the signals generated by the brain neural cells and they reflect different of brain's electrical potentials. These signals were used in starting from the past decade mainly to study information dynamics of brain neural. Behaviour and dynamics of the brain are diagnosed for the goal of brain disturbances discovery [1]. These signals are time series signals having a nature of low frequencies and tend to be highly sensitive to other electrical surrounding fields. They are recorded with the help of specialized isolation means of skull helmet consisting of many nodes. These nodes or electrodes are attached to a specific distribution of positions on the head, wet or dry [2], [3].

EEG signals due to their nature, and in order to get rid of different signals interfere them, are recorded and stored with specialized data formats in a huge amount, if we talk in term of data arrays, then they can have millions of rows for only few minutes of acquisition. As though, the traditional visualised data analysis methods do not help well with understanding them, especially if we know that EEG signals are highly with error rates and contamination with interfering and disrupting signals and we need different methods to deal with these issues.

Data processing techniques like regression, classification, statistics, data cleaning and reduction, etc. along with different other techniques like machine learning and deep learning can play a vital role in the goal of studying and getting good insights of these signals. EEG signals processing and exploitation can be employed using various techniques results for solving the now days issues like in medical care systems or patient rehabilitation device, forecasting different human emotional and mental conditions [4], [5]. Besides, they can be used as promising technology in a way for controlling or decision making devices for interactive real time, virtual and augmented reality as input nodes in fields like entertainment or military [6]. The previously mentioned studies have been reported to using MRI imaging (Magnetic Resonance Imaging) that uses the means of studying and investigating brain activities noninvasively of the anatomical images nature [7], [8]. The MRI imaging was widely used but because of different reasons like it's limited temporal resolution, even it shown a high spatial one in the measured data signal, which is driven by the fact that it is affected negatively by the blood BOLD attribute (oxygenated level dependency), which can be avoided by deploying the desired analysis using EEG recorded signals techniques [9], [10].

Both fields of sports and exercise studies were not commonly discussed using EEG, just like the Psychology, they were widely submissive to the use of MRI till the near past [11], then EEG signal analysis as a technique started getting more attention in both fields, like those related with the changes in EEG signals after performing cycling exercises with different intensities [12], [13]. Recently, EEG recorded signals motivated by the human body different activities, biological and physical, used as a human body vital activity monitor system. Neuroergonomics as example got more interest recently in the studies that discuss brain potentials and activities for people that participate in various sport and day life activities [14].

Among those vital body signs, we chosen a one that we expect to get promising results in the goal of foretelling the lactate enzyme level in the human body that whenever increases, it gives a sign about the body tiredness increase level. This goal is to be studied by validating these enzyme levels in contrast to changes encountered to EEG signal recordings, when compared between two states of exercise, before doing single shot of acute exercise and after doing the exercise Getting insight from a good idea proven by studies [15], [16], the lactate enzyme level could be increased to the peak value after performing an exercise of the type maximal treadmill run within short time window.

1.1 AIM OF STUDY

By the concept of our study, we set our aim to present a methodological framework called Physical Tiredness Classification System (PTCS), to be utilised for the identification of human physical tiredness status. By this concept, we divided the work into two parts, in the first one we discussed the system ability to differentiate between two classes, tired or low-tired, while in the second part the differentiation between tired, moderate-tired, and very-tired classes was discussed. These levels could be reached by motivating the brain's electrical activities by exercise. The exercises are directed to affect the resting state signal by performing single bout of acute exercise.

Next, the brain recordings are passed over two different feature extraction methods, frequency band power and time series sample entropy. These feature metrics are applied to a short length window, typically of 1 second from the brain EEG recordings. The achieved results show successfully predicting of the intended measure before and after performing a single moderate bout of acute aerobic exercise, which is a novel to the best of the author's knowledge in the literature. Classification results shows a high score with the proposed methodology when applied to our unique data set and compared to the results of the same classification methods used by other studies in the literature in term of different classification measures like accuracy, precision, recall and F1- Score as we well discuss them in the next chapter.

1.2 LITERATURE WORK

Machine learning has been applied to EEG data in many studies. Such a process usually involves an artefact removal step, a feature extraction step and classification as the final step. Recent research has reported advancements in automating the artefact removal process using unsupervised machine learning as well [17]. The features extraction and classification process of EEG signals has been used for tasks such as seizure detection [18], mental work load detection [19], sleep studies [20], emotion detection [21], motor imagery [22], and neurodegenerative features detection such as fatigue [23], Attention Deficit Hyperactivity Disorder (ADHD) [24], [25], and anxiety [26]. Studies showed preference of using Support Vector Machines (SVM) as a machine learning algorithm able to achieve accurate results in EEG analysis [27]. The use of EEG as a technique of analysing in most of the above-mentioned fields has been applied for a long time in many studies. The advancement in computing has also offered the availability of using artificial intelligence and machine learning in these fields. However, using EEG in the field of exercises and sports was not common until recent times. The fact that such application has not made as much use of machine learning techniques as other EEG application in the literature is also noteworthy [28]. With regards to research done on EEG and exercise, a study investigated the impact of severe physical short-term exercise and long-term workout training on the EEG resting-state alpha frequency (iAPF) of the individual, participants had performed a protocol of steady state exercise (SSE) or a protocol of exhaustive exercise (EE), on two separate days. EEG signals were recorded for 2 minutes before performing the exercise followed by immediate recording after the exercise, as well as after a period of rest for 10 minutes. To investigate whether an improvement in physical fitness modulates the resting state iAPF response to an acute bout of both exercise types, all calculations were done again after four weeks of training. Results shows that following EE ($P = 0.012$), the iAPF was significantly increased, while following the SSE it did not increase [29].

In another study, it was desired to discuss the possible changes in mood and EEG activations after performing three levels of intensity running exercise; low, preferred and high. A 5 minutes of each EEG recordings were made before, directly after and 15 minutes after the exercise trials. The high intensity exercise was found to affect both EEG and the mood of the subjects [10]. It showed an increase in alpha ($\alpha 1$ frequency: 7.5–10 Hz) and a decrease in beta ($\beta 1$: 12.5–18 Hz) frequency. Brain activities during performing an acute aerobic exercises were examined and found to be increased[11]. The experiment was divided into three stages, adaptation, exercise, and recovery. In the first part, participants were asked to sit down quietly for 10 minutes, in the second part they were asked to perform a moderate-intensity 15-minute cycle ergometer exercise, and in the last one they had a recovery period of 10 minutes. The EEG data was collected during the last 2 minutes of each stage and the power densities across both alpha and beta frequencies were combined and observed. The results showed that the brain activations had increased, i.e. beta frequency band power was increased, while the alpha frequency was decreased during the exercise and then returning to the power baseline after completion the exercise and recovery periods.

The absolute power changes in EEG after conducting an acute exercise was investigated to discover the possible changes. The study intended to study variations encountered at the beta and alpha frequency bands after a maximal effort exercise of cycle ergometer was made by [12]. Experiments were applied with the participation of ten young healthy volunteers, 4 men and 6 women aged between 25 and 30 years. They first take a relaxing period of 10 minutes and then the EEG recording of the first experiment session of 8 minutes done while they were sitting with a calm fashion on a comfortable wide chair to reduce muscular disorders and data was used to represent pre-exercise. Then the participants were required to perform a cycle ergometer with a progressive workload. The exercise session ends when the subject performed the maximal effort test and feels exhausted based on a rate of perceived exhaustion protocol that measures each subject’s state of fatigue. Then the post exercise EEG data recording began immediately with returning to the calm fashion of sitting on the same chair for another 8 minutes. The findings demonstrate observed increase in cortical activation represented by a significant increase of absolute power in beta frequency at Fp1, F3, F4 and C4 electrode areas.

Increasing pace of exercise intensity and its effect on the EEG activation was studied by [30], along with the effect on the lactate enzyme concentration in blood. In this study, 19 subjects had participated in this study, 17 of which were men. Participants were aged around 42 years with an obvious healthy state. They conducted, on separate sessions, six stages of run with increasing velocity at each successive stage. Each stage lasted 6 minutes, with a rest period of 2 minutes between stages. The EEG measurements were taken along with the lactate enzyme blood concentration at different time points. The 2 minutes EEG recordings were taken before the starting of the experiment, after each stage of velocity increment and twice after finishing the exercise, one after 15 minutes and another after 30 minutes. Using the same protocol, the measurement of lactate enzyme concentration in the blood was made. The results show that exercise induced significant spectrum power changes of EEG at every position of each electrode. Also, the increased intensity of exercise induced significant changes in lactate concentration, even after a 15 and 30 minutes from the exercise finish time, the levels were still higher than the baseline.

In a good study of the literature [31], the effect of exercise on cortical activity and therefore concussion evaluation tools and tests was studied. EEG recordings, heart rate and arterial oxygen levels were collected before and after a set of healthy volunteers performed a one-mile run. EEG activity was shown to have decreased in the theta band (4-8 Hz) during both EC and eyes open resting periods. Additionally, the EEG showed a shift to higher frequencies during the Sport Concussion Assessment Tool (SCAT3) balance assessment, as well as a slowing effect during the King-Devick test (K-D test) which evaluates impairments of eye movements, attention and language function. All of which led to the conclusion that concussion evaluation tests can be affected by exercise, and therefore care while taking such tests should be made.

To study the effect of low intensity acute aerobic exercise on EEG, subjects in another study were exposed to a stress experiment by listening to an unpleasant 5 KHz tone and/or perform mental tasks while their EEG signals were being recorded [32]. The stress experiment caused a mean reduction of the low-alpha amplitude of the EEG signal by 20%. After a 20-minute acute exercise of low intensity, the EEG signal was taken again and showed increase in the mean amplitude of both low-alpha (more than 30%) and theta bands, which suggested that such exercises help in recovering low-alpha waves. No significant changes were found in the beta and gamma bands as a response to the stress experiment or the exercise.

To determine the effect of exercise on the reliability of the connectivity of brain networks, a group of male participants' EEG was recorded before and after submaximal exercise twice within one week in another study [33]. After the Small World Index (SWI) and other graph measures were constructed using the Weighted Phase Lag Index (WPLI) and spectral coherence. From the graph measures, the Intraclass-Correlation-Coefficient (ICC) and Coefficient of Variation (CoV) were calculated as reliability indicators. The ICC values showed that connectivity was positively affected by exercise, having increased from poor to good before exercise and from good to excellent after exercise. The study concluded that post-exercise EEG signals results are reliable to measure changes in the brain network originating from exercise.

In [34], the effect of intense cardiovascular load on intensity dependent modulation in brain network efficiency was studied. EEG signals were collected from 16 trained participants required to perform an incremental treadmill exercise. Before the exercise and after each stage resting-state EEG signals, biomedical indicators among which blood lactate levels (Bla) is, as well as Borg scale were taken. After deriving the small world index (SWI) from the EEG signals in the theta, lower-alpha and upper-alpha bands, efficiency of the brain network was evaluated, showing a reduction in the theta band, whereas the lower-alpha and upper-alpha bands showed no significant difference in the brain network efficiency metrics used.

In a quantitative review, 18 studies done on a total of 282 participants were reviewed. Effect of recording site was found to be not significant to the outcome of the results. In addition to increase in alpha frequency, increase in beta frequencies was also observed, leading to a conclusion that the change in electrical activity of the brain during or after exercise is not specific to a frequency band nor to a hemispheric location [35].

To determine the effect of exercise on the resting state EEG signal of children with ADHD, two groups of children with ADHD were asked to undergo different eight week plans in [36]. The first group consisting of 15 children participated in an eight weeks long water aerobic exercise program, whereas the other group of 14 children were asked to refrain from participating in exercises programs as well as vigorous exercises. The parents and teachers were required to fill in a Descriptive Behaviour Disorder (DBD) scale which helped identifying the ADHD subtype of the children. The children were recruited from different subtypes of ADHD (predominantly inattentive, predominantly hyperactive and combined). For eight weeks, the exercise group conducted water aerobic exercises lasting 90 minutes twice a week. Resting-state EEG with eyes open was collected before and after the start of the program from both groups. Nine electrodes were used with three electrodes on each of the central, parietal, and frontal areas. After the spectral powers of each electrode's EEG signals were found using FFT, average power of each area was calculated. Additionally, mean theta/alpha and mean theta/beta frequency powers was calculated for each region. The results of the study showed that the exercise group showed a reduction in the central and frontal theta/alpha ratio. Since high theta/alpha power ratios may indicate reduced executive functioning and self-control and delayed maturation, the reduction after the exercise period lead to concluding that exercises may improve cognitive functions in children with ADHD.

In order to identify the areas of the brain affected by exercise and relate these changes to the individual's exercise preferences, physiological indicators as well as 5-min EEG were taken from eleven participants before and after three different types of exercises, namely incremental treadmill run, arm crank and bicycle ergometer. The EEG signal was then used to form the standardised Low Resolution Brain Electromagnetic Tomography (sLORETA). It was found that all exercises increased the beta activity in Brodmann area seven. Additionally, while the EEG signal obtained after 15 and 30 minutes of the treadmill and bike exercise resulted in decrease of the frontal brain activity and increase in the occipital activity, the same pattern was not noticed in the arm crank exercise, which suggested that different exercises affect the brain activities in different ways [37].

As for applying machine learning in the exercise-effected EEG analysis [38], performed feature extraction of EEG signals during exercise induced fatigue. Initially, a group of volunteers were subject to a static exercise aiming to measure the maximum voluntary contraction (MVC) of the quadriceps muscle. Afterwards, while having their EEG signal recorded, subjects were asked to perform a dynamic exercise that should drive the quadriceps muscle to fatigue, by repeatedly moving their knee joint at a metronome's speed. The test continued at the metronome's frequency until participants reached fatigue state and could not extend the knee joint after verbal encouragement. Subjective fatigue metrics such as Stanford Drowsiness Scale and Borg Scale were taken from the participants before and after the dynamic exercise. The EEG recording process used 19 electrodes covering all four lobes of the cortex. Later on, 80% of the EEG data was used for training an SVM algorithm, whereas 20% was used for testing. After making use of Multivariate Empirical Mode Decomposition (MEMD) and Hilbert-Huang algorithm, a better accuracy was achieved (90%) was achieved compared to using SVM.

To investigate the effect of exercise on motor memory, a group of 25 subjects went through four sessions in which they were asked to perform an isometric hand gripping session. The subjects were divided into two groups, the first was required to go through a 15-min intense cycling exercise, whereas the second group were asked to rest. EEG recordings were taken from subjects before the exercise/rest period and immediately after the period as well 30 minutes, 60 minutes, and 9 minutes after the exercise. Afterwards, topographical maps were formed from the analysis pipe. The study's findings show that exercise does improve the motor memory. In addition, the deep learning algorithm superseded common statistical methods in terms of the range of the frequency used, since it revealed discriminative spectral features in a band of 2 Hz (27-29 Hz) as compared to the (15-30 Hz) of statistical methods [28].

The effect of physical activity on the performance of university students was analysed using a model based on two EEG parameters (spectral power, signal entropy) and students'' response time. Six students' EEG was taken while performing a Psyco-Motor Vigilance task from which their response time was measured. Afterwards, students attended a 20-minute lecture. Next, depending on the assigned task, students were either asked to silently read a scientific article for 10 minutes (control) or asked to perform physical activities for the same period of time (experiment). The students right afterwards repeated the same 15 minutes Psyco-Motor Vigilance task with their EEG being recorded. Using the proposed classification model, seven different algorithms were applied. The statistical results showed that students who had physical activity break showed an improvement in terms of response time, whereas no significant changes were found in the control subjects. As for the classification model, among the algorithms used artificial neural networks (ANN) and MVC were the most successful, with an F-1 score of 88% and 85% respectively [39].

From reviewing the literature, studies that have used machine learning in order to detect fatigue from EEG signals generally either focus on mental fatigue or driving induced fatigue [15], [26]. In [40], the authors proposed a system that takes into consideration the non-linearity of EEG signals to detect fatigue. The proposed system was intended to use approximate entropy and sample entropy as measures of complexity of the EEG signal. 50 volunteers were required to seat themselves at a distance of 1 meter from a screen while their EEG and Horizontal and Vertical Electrooculography (HEOG & VEOG) were recorded. The EOG signal was used along with EEG readings as part of a manual drowsiness detection process. Using relevant scales, the participants' subjective SSS scale (sensation seeking scale) & Karolinska sleepiness scale, and subjective fatigue (Samn-Perelli checklist, Li's subjective fatigue scale and Borg's scale) was measured. Afterwards, participants were exposed to a stimuli rich driving simulation experience of 15 minutes that was supposed to provide alert state EEG recordings. After collecting the alert EEG signal for 15 minutes, the participants started a driving simulation on a generally straight roads with few cars in a continuous fashion. This straight driving stage continued for 2-3 hours, until EEG indicated drowsiness/fatigue. Once fatigue stage was reached, the participant continued to drive 15 minutes more, and the EEG signal of this last 15 minutes was considered as fatigue/drowsy EEG. This signal was further pre-processed by labelling the alert and drowsy EEG by a psychophysiologist, using blinking shown from EOG (drowsiness blinking period lasts more than 0.5s) and the EEG signal's dominant frequency, with alpha component being dominant during drowsiness. The results showed that fatigue EEG has less complexity (Sample Entropy and approximate Entropy) than alert EEG. Additionally, this difference was more noticeable on parietal and occipital areas. When 4 channels situated in these areas (P4, P3, Pz, Oz) were chosen for further analysis of classification using combined entropy's results, the used SVM algorithm showed average accuracy rates between 88.92% in electrode Oz and 91.28% in electrode P3, the later had significant differences between two states is 0.022 for approximate entropy and 0.026 for sample entropy. P3 electrode showed the highest sensitivity (93.67%) yet a relatively small specificity (88.89%). The highest specificity was reached at electrode P4 (91.11%).

1.3 ANATOMY OF THE BRAIN

The brain is one of the most complex systems, if not the most complex one in the human body. Unable to fully understand itself, it represents billions of neurons connected to each other responsible for several cognitive and controlling functions.

The brain occupies the most important part within the central nervous system, which is consist of main three parts, the brain itself, the spinal cord and the brain stem which connects the previous two parts. In the next section, we will discuss anatomically the brain's main parts.

1.3.1 Major Parts of the Brain

Anatomically, the brain consists of three major parts, namely the cerebrum, the cerebellum, and the medulla oblongata. The cerebrum is responsible for voluntary actions as well as thinking, reasoning and receiving sensory information from sensory nerves across the body. It consists of a cortex (gray matter) and an inner layer (white matter). The cortex is further subdivided into several lobes and will be discussed in the next section.

1.3.2 Lobes of the Brain

The brain’s cortex can be divided into four main lobes, the frontal, parietal, temporal and occipital lobes. The frontal lobes are the largest of all lobes and is located in the frontal part of the cerebrum. It responsible for prospective memory used in planning, speech and language and movement control. The parietal region is posterior to the frontal region, and is functionally divided into two areas: The anterior parietal lobe and posterior parietal lobe. The anterior parietal lobe receives sensory signals from the thalamus and is responsible for interpreting somatosensory signals (touch, temperature, pain etc.) due to the fact that it contains the primary sensory cortex. The posterior parietal lobe is further divided into two lobules, the superior and inferior parietal lobules. The earlier being responsible for high order functions such as motor planning, whereas the later contains the secondary sensory cortex which integrates somatosensory inputs from different regions of the brain with other modalities to perform complex functions [41].

Although results from functional mapping show that the body is fully represented in both the primary and secondary sensory cortex, the map of the body in the secondary sensory cortex is thought to be less precise [42].

The temporal lobe is the second largest and is responsible for many functions. Anatomically it is divided into a lateral temporal surface and a median temporal surface. The lateral temporal surface contains several regions that perform functions related to auditory functions, semantic memory, language, speech, and visual and facial perception. The medial (mesial) temporal lobe is a memory system responsible for declarative memory. Research is on-going on which part of the medial temporal lobe is responsible for which subtype of declarative memory, such as familiarity and recollection [41], [43]. The occipital lobe lies in the most posterior part of the cerebrum. It is the smallest of the four lobes of the brain and is responsible for visual processing since it contains the visual cortex.

1.4 ELECTROENCEPHALOGRAM (EEG)

To avoid the surgery operations, there are four possible non-invasive ways by which the brain recordings can be measured namely: (EEG) electroencephalogram, (fMRI) functional magnetic resonance imaging, (fNIRS) functional near-infrared spectroscopy, and magnetoencephalography (MEG). Although other techniques are available, but for a couple of reasons like the low cost, good temporal resolution and ease of portability, the EEG is dominated for usage with many different applications like Brain Computer Interface (BCI) [44]. EEG signals represent the recording of the electrical field signals over the scalp generated by the brain neurons. These recording only matter if they were generated with enough potentials and are amplified later on for reasons of display [45]. These signals have a range of 1 Hz up to around 100 Hz and an amplitude ranging between 10 μV and 100 μV which makes them very sensitive. They are naturally non-linear and non-stationary and require a special signal processing techniques to get useful information from them.

Although EEG is originally meant to measure the scalp electrical potentials as a reflection for the electrical activity of the brain, recent advances have allowed to use EEG to reverse the problem, i.e., to generate an electrical map of the brain showing current densities. An example of such is the Low Resolution Brain Electromagnetic Tomography (LORETA) [46].

1.4.1 Frequency Spectrum of EEG

Frequencies of the EEG signals are divided onto five bands, namely Delta (0-4 Hz), Theta (4-8 Hz), Alpha (8-12 Hz), Beta (12-30 Hz), and Gamma (30-60 Hz) bands [47]. The division of frequencies into these bands is a result of the limitations of the pre-computer era the continued later on. The range of each band however may not subject to consistency, and may vary depending on the machine used and its built in filtering and definitions [48]. In figure 1.1, the frequency bands in time domain are shown.

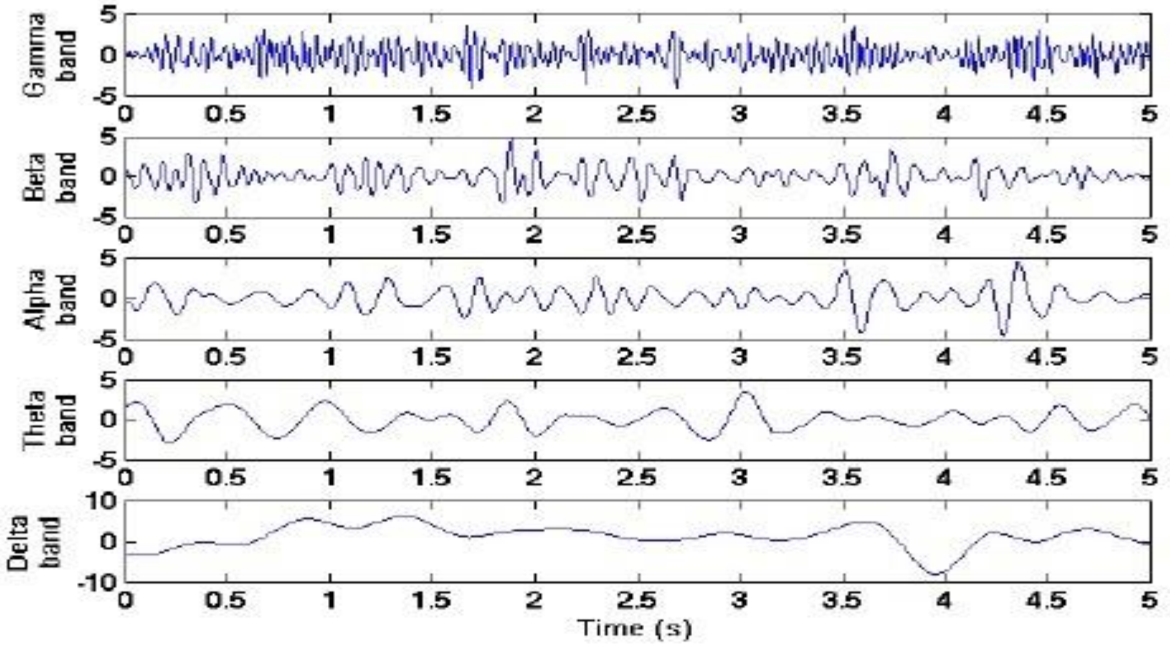

Figure 1.1: EEG Frequency Band Components in Time Domain [49].

1.4.2 Frontal Lobe and Its Theta Activity in EEG

As previously mentioned, the brain’s frontal lobe is responsible for several vital functions. The fact that the frontal lobe has cognitive functions and higher order control functions and that these functions' relationship with theta frequency rhythms has been discussed in the literature can lead to evaluating high powers of theta frequency spectrum in the frontal lobe as an indication of cognitive activities [50], [51].

The effect of exercise on such frequencies has been previously referred to in the literature review section. Studies have shown both reduction in [31], [34] and increase in [32] of theta activity as a result of exercise. The fact that the type of exercise does affect whether an increase occurs or not has been shown in [37] and [51].

1.5 EEG AND RESTING STATE

EEG signals are generally taken during resting state. In such an arrangement, electrodes are placed on the subject's scalp, with distances between them set according to certain distribution (such as the international 10-20 system). The resting state EEG and its features is discussed in the next section.

1.5.1 Characteristics of Resting State EEG

EEG measurements are usually done in a resting state with either eyes open or eyes closed states, although some studies have reported using EEG during driving [40] and exercise [33], [51]. Resting state EEG consists of a mix of the previously mentioned low amplitude mixed-frequency background rhythms, where each electrode (channel) attached to the scalp may produces a different signal that electrode attached to the scalp may produces a different signal that consists of a mix of these frequencies.

A 16-channels EEG signal is shown in figure 1.2. During eyes closed EEG, alpha rhythm is dominant, therefore it is also termed posterior dominant rhythm and is attenuated with the opening of the eyes. The rhythm is characterized by symmetry across the two hemispheres in the normal individual and may have many variations based on location and the individual himself, such as temporal, frontal, and paradoxical alpha rhythms as well as mu rhythms. Beta rhythms are lower in amplitude and are generally considered a sign of drowsiness. Theta and delta rhythms are considered a drowsiness sign as well and are also associated with response inhibition [51]. Theta rhythms and their frontal lobe activity in particular were discussed in section 1.4.2.

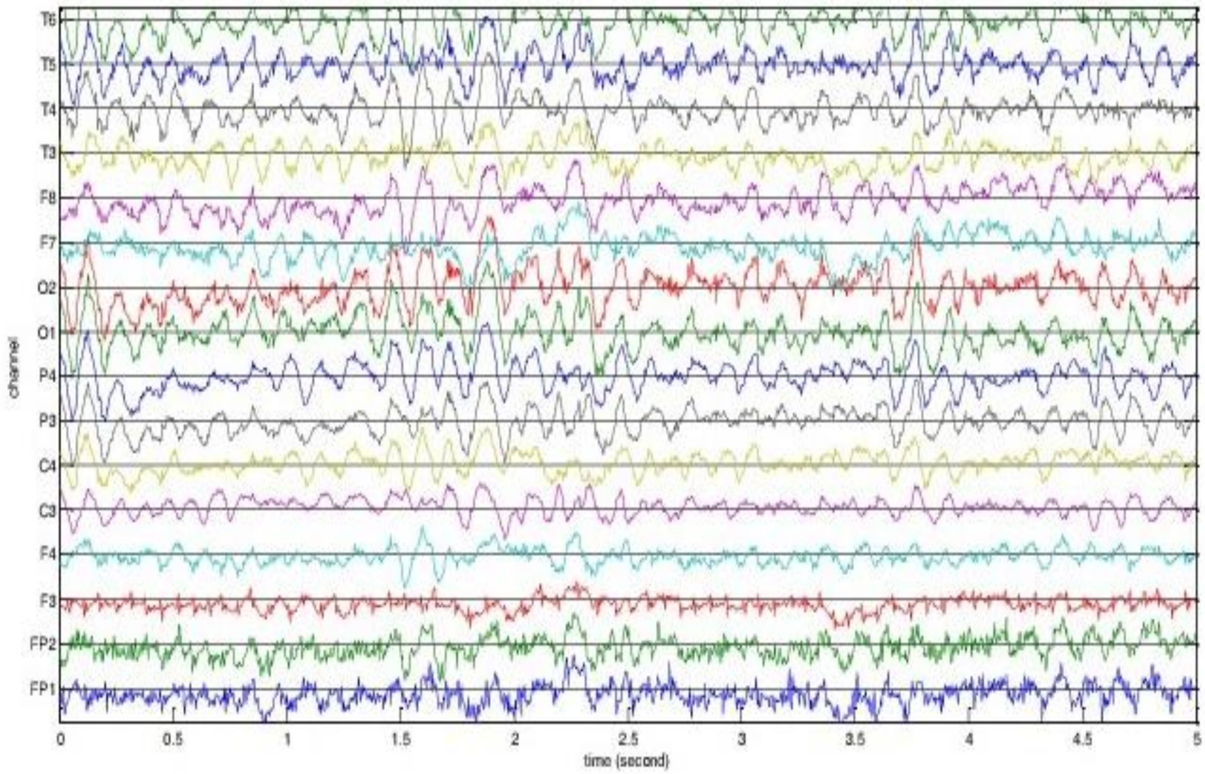

Figure 1.2: 16 Channels EEG Data [52].

1.6 EEG IN THE TIME AND FREQUENCY DOMAIN

EEG signals are nonlinear time series signals composed of many frequencies. The analysis of such signals can either be done in time domain or using the frequency domain after applying suitable transformations. In cases of time domain analysis, non-linear techniques such as delay differential equations (DDE) [53], sample entropy and approximate entropy [40] are employed. In case of frequency domain analysis, the signal needs to go through a suitable frequency transform algorithm. The frequency analysis allows to analyse the power of different frequency bands in the EEG spectrum, which gives insights on several physiological and psychological matters. Spectral power analysis is commonly used in analysing EEG signals as it provides an easier method of analysis. The necessary time-frequency transformation process is discussed in the next section.

1.6.1 Frequency Decomposition of Time Series EEG

Several techniques are available for converting the time domain information into the frequency domain. Generally, these methods offer a trade-off between temporal resolution and frequency resolution. That is, the larger the epochs (time windows) taken for the transformation process, the greater the frequency resolution but the poorer the temporal resolution. Among the techniques that can be implemented for frequency transformation are Fourier Transforms, discrete and continuous wavelet transforms, Hilbert-Huang transform and matching pursuit [54]. Using Discrete Fourier Transform (DFT) and its variation Fast Fourier Transforms (FFT), the signal in frequency domain can be easily obtained. Fast Fourier Transform is explained in the next section. Wavelet transform is a transform that uses a variable window size across different frequencies, thereby overcoming a main drawback of transforms that use fixed windowing which is the fact that they capture the global spectrum with a specific resolution. A wavelet transform is able to capture localized frequencies of a signal. Applying a wavelet transform requires choosing a base wavelet such as Haar wavelet or Daubechies wavelet. The fact that wavelet transforms capture localized frequency components makes it particularly useful for analysing signals containing temporary frequency components such as Electrocardiogram (ECG) signals. Applying wavelet transform for biological signal processing requires choosing a biologically plausible base wavelet. For the purpose of EEG, the Morlet wavelet is among the most commonly used base wavelets [55].

1.6.2 Fast Fourier Transform FFT

Fourier transform is a mathematical transform that makes use of the fact that any signal can be decomposed into a sum of sinusoidal signals with different frequencies and amplitudes. The Discrete Fourier Transform (DFT) is a version of the Fourier transform that is implemented to transform discrete and periodic signals. Particularly, the DFT of a discrete time signal can be computed as per equations 1.1 and 1.2.

$$Re\, X[i] = Sigma\, x[j] \cos(2\pi \text{ i j/N}) \tag{1.1}$$

$$Ime\, X[i] = Sigma\, x[j] \sin(2\pi \text{ i j/N}) \tag{1.2}$$

where $Re\ X$ is the real part of the frequency spectrum, $Ime\ X$ is the imaginary part of the frequency spectrum, N is the number of samples of the discrete time signal, j is the discrete signal's sample number, i is the discrete output's sample number.

The computational complexity of the DFT can be represented as O(N^2), which indicates that the complexity exponentially related to the length of the signal (N). It is possible to reduce this complexity into O($Nlog2\ (N)$) using the FFT thereby increasing computational speed drastically [56].

Fast Fourier Transform (FFT) is a computationally efficient and modified algorithm. It uses the fact that the DFT of a signal of length N can be rewritten as the DFT of two signals of lengths $\mathrm{N}/2$, one containing the even points and the other containing the odd points. If $F(y)$ represents the FFT of the function $f(x)$, then FFT is defined as in equation 1.3.

$$F(y) = \sum\nolimits_{x\ even} f(x) w_x^{yx} + \sum\nolimits_{x\ odd`} f(x) w_x^{yx} \tag{1.3}$$

for $y = 0, \ldots..,\ X - 1,\ \ X\ even$ and $X\ odd$ are corresponding to the even and odd EEG sample of $f(x)$ function, $w = exp(-2xj/X)$ where j is the imaginary fraction and $X = 3.14$.

1.7 TIME SERIES AND ENTROPY

Time domain analysis of nonlinear time series signals such as EEG signals require the usage of methods able to deal with the non-linearity. Entropy is a measure of repeatability and predictability (and therefore uncertainty) in a signal [57], [58]. The several types of Entropy and the procedure to calculate the Sample Entropy (SE) for EEG signals are discussed in the next sections.

1.7.1 Entropy and Its Types

Entropy has several types, including Approximate Entropy (AE), Sample Entropy (SaEn), Differential Entropy (DE), Permutation Entropy (PE), Fuzzy Entropy (FE) and Multiscale Entropy (MSE). AE was first developed by Pincus in order to analyse complex and nonlinear systems. It was meant to measure regularity in time data series, particularly those with stochastic components [59]. By tuning two parameters, namely the number of data points to compare (m) and a filtering level (r), a model independent measure of regularity can be reached.

SaEn was designed with the capabilities to overcome issues that AE didn't. First, AE does not guarantee a relative consistency. Second, its result depends on the data series' length. SaEn on the other hand provides relative consistency and is generally independent of the length of the signal. The method of calculating SaEn is discussed in the next section.

1.7.2 Calculating Sample Entropy

SaEn was developed as an improve of AE, and the function of it represents a negative representation of logarithmic that two time series sequences of the length m of certain data type points stay similar for the next m+1 points can be calculated using the next shown in equation 1.4

$$\mathrm{SaEn}(\mathrm{m},\mathrm{r},\mathrm{n}) = -\ln\left(\frac{X}{Z}\right) \tag{1.4}$$

values of X and Z are defined as follows in equations 1.5 and 1.6:

$$X = \left(\frac{[(n-m-1)(n-m)]}{2}\right) X^m(r) \tag{1.5}$$

$$Z = \left(\frac{[(n-m-1)(n-m)]}{2}\right) Z^m(r) \tag{1.6}$$

In this context, $X^m(r)$ is the possibility that the intended two signal or data sequences stratify for $m+1$ of points, and $Z^m(r)$ is the possibility that the wanted two signal or data sequences stratify for m of points, the length of sequences to be compared is m, and r is the value of tolerance for accepted matches, n is the length of time series data. The choice of m and r is not a subject of consensus for short biological data sets.

Yet in clinical data, and by many studies, values of m and r gives better statistical validity within specific ranges. For m, it is commonly set to either 1 or 2, while r tuned between 0.1

and 0.25. As though, in our study we set m value to be 2, whereas r is chosen to have 0.1 value of the standard deviation of the entire data set [58], [60].

1.7.3 Sample Entropy of EEG

Entropy analysis for brain signals unveils the complexity of the signal under study. It has been utilized for several fields such as consciousness level analysis and prediction, emotion recognition, aging brain analysis and quantifying the processing of information within the brain's network. Such applications have shown promising results opening new research opportunities.

Sample entropy analysis of EEG is coupled with Multivariate Empirical Mode Decomposition (MEMD), a process used to decompose a complex time series into intrinsic mode functions (IMFs), which define upper and lower envelopes in which all data should lie [61], [62].

2. MATERIALS AND METHODS

In this chapter, it will be talking about the type of data which have been used in our proposed system work, the way it was collected, the data cleaning procedures applied during the experiment steps. Besides that, the pre-processing methods applied to clean noises, artifacts and other extreme undesired signals encountered during the signal acquisition process is discussed. Furthermore, it will discuss the feature sets which have been extracted and fed to classification models, along with explanation of each classifier used during the work. The lactate enzyme is explained in the last few pages of this chapter showing its role and the levels reported during the experimental steps. Finally, the proposed prediction system is explained with explainer paragraphs showing the technical components and procedures.

2.1 EEG DATA

The data used for the study purpose of this dissertation was collected and provided from the side of Assoc. Prof. Dr. Adil Deniz Duru (co-advisor of the thesis, Ethical Review Board of the faculty of Sport Sciences, Marmara University), available through a reasonable request. The following section shows the way by which data were collected. During the intended experiment, and before performing acute exercise, measurements represent the lactate enzyme level were collected from 9 members of elite level karate athletes from Turkish national team. These lactate measurements represented the initial physical status of subjects and were assigned as a not-tired state indicator of the participant [10]. These measurements were found and reported to have low values at the baseline, around 2 millimol/L as reported and approved by the Ethics Committee of Medical Faculty, Istanbul Arel University, by the document numbered (2016-06).

Before doing the exercises related to experiment, subjects have been asked to close their eyes and rest on a chair for 3 minutes steadily and quietly while not thinking about anything as possible. Then they are asked to perform a test of Backward Digit Spanning by selecting any three-digit number and start subtracting a 1-digit odd number, number seven for example. The data collecting procedure begins by using EEG data acquisition tools, BrainAmp amplifier of a 1000 Hz sampling rate attached to 16 channels of the subject’s brain, namely Fz, Fp1, Fp2, F3, F4, Cz, C3, C4, T7, T8, Pz, P3, P4, Oz, O1, O2 with a dry type of electrode caps. These initial EEG recordings are measured and reported representing not-tired class (low-lactate enzyme).

The next step is to measure the second class that represents semi-tired state of the subjects. Every subject is ordered to perform in separate sessions an acute exercise of short time. What distinguishes these exercise sessions is that they are of a moderate intensity. They are done by doing 20m Shuttle run test, which is an exercise of an incremental pace used to find out the human's body maximum oxygen consumption ability. It is very important measure to test the aerobic endurance of athletes and involves running for a distance of 20 meters while running pace increases, meanwhile the time allotted for each run decreases as the test stages in progress [63].

The Rated Perceived Exertion RPE test is used at this stage to evaluate the subject's tiredness level. It is achieved by asking the subject, without interrupting the exercise, about his or her level of tiredness they feel have been reached [64].

In the next stage of the experiment, subjects had taken a 1-minute resting period followed directly by further four lactate enzyme measurements successively every 2 minutes. These measurements were found to have higher values than the previous ones made in the first stage. These measurements were found to be between 4 and 5 millimol/L. In the meantime, following to lactate measurements, EEG signal acquisition was made with keeping eyes closed condition for 3 minutes. These recordings were saved and assigned to be reflecting a state in which, subjects have reached a certain tiredness condition, at which they start feeling a moderate tiredness level. This stage of experiment reflects a semi-tired level at which subjects report a higher level of tiredness by RPE test. As the exercise advances, subjects reach a level of tiredness and they start reporting level 16 of RPE test in agreement with BORG scale, which means that they got exhausted and feel a need to get rest [65].

Following a 1-minute period of resting on a chair, a group of more four lactate enzyme tests were made with 2 minutes separate period between them. Measuring lactate enzyme levels at this stage was found to report high values between 10 and 14 millimol/L. After that, and with eyes closed, EEG signals recordings were collected for 3 more minutes. These measurements will denote another subject's physical tiredness level related with lactate level, reflecting very tired class.

The recorded EEG signal are highly contaminated time series data and very sensitive, because they encounter artifacts and noise caused by different body and facial muscles movement or eye blinking. Therefore, and before doing any data processing task, prior to and after-exercise data were considered for artifact removal and noise cleaning pre-processing techniques in the goal to get clean and organized data. This includes removing unwanted data epochs, especially those of extreme values which exceeds amplitude more than 100 μv in some channels. Band pass filtering is one of the signal pre-processing techniques used to achieve band pass filtering goal and the resulting clean data was provided to the next experimental stage.

In the first phase of the work, we had used the data that represent only two of the three classes denoting and trying to differentiate between tired or not-tired status of the subjects (lactate level high or lactate level low), while In the second phase we tried to classify between all the three classes we had on hand, not-tired, semi-tired or very-tired that reflects one of the subject's physical status.

2.2 PRE-PROCESSING EEG RAW DATA

As the recorded EEG data had a high artifacts and noises value, they must be cleaned and organized in a form suitable for the next stages in the proposed system using pre-processing techniques. The applied pre-processing techniques had utilized the EEGLAB tool kit version 2019.0 attached with the MATLAB software version R2018a. First of all, the data recording was saved in a form of (.eeg) files, which are a special MATLAB data structure that contains all the related information of current EEG data container (dataset). So, we have firstly imported the raw EEG data by specifying the computer's driver location in which (.eeg) file was stored. After loading the data, the first thing to do is removing the linear parts from the signal, which will remove the baseline data from all the data channels included within recordings. This will make data free of the DC offset before performing any filtering, otherwise it is going to make artifacts at each channel data [66].

The data pre-processing continues by applying high-pass filtering to data with 0.5 Hz frequency boundary, as it is necessary to give a good quality data. Besides, the low-pass filtering is also applied at 50 Hz frequency boundary to remove high-frequency noises from data. The data may encounter extreme signals in some channels that have more than 100 Hz frequency values and should be removed entirely as they do not refer to any useful EEG data. Furthermore, data can be contaminated with undesired periods of distortion caused by some human mistakes during experiment or electrodes misconnections. They appear in a form of scrambled signals that lasts for a few seconds within the data plotted using the Channel data(scroll) function from Plot menu tool in the application as shown in figure 2.1 below.

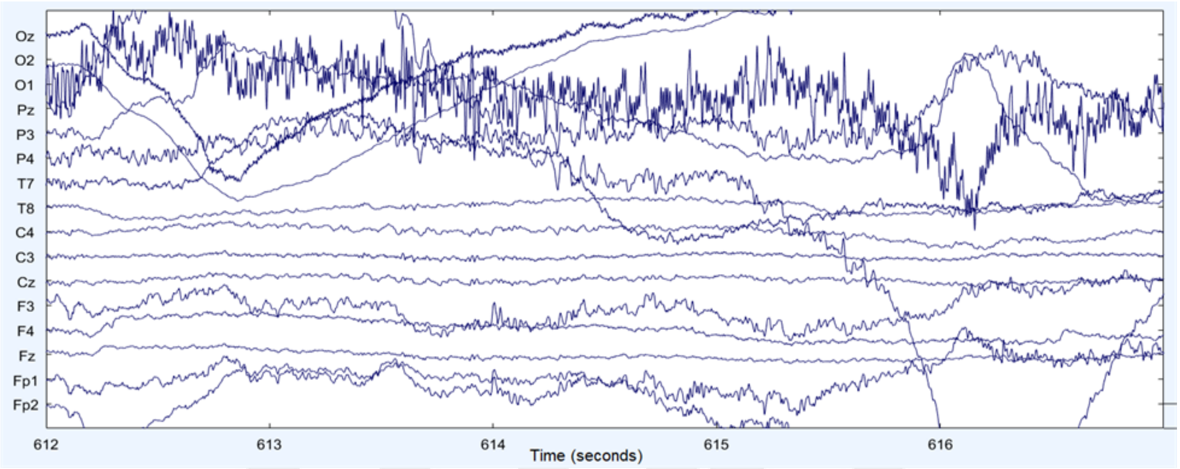

Figure 2.1: Sample 5 Seconds of Contaminated EEG Data.

After performing the required signal pre-processing steps, we will get a clean and semi error free EEG recordings as shown in figure 2.2. Now, the corresponding data are arranged to form a 2-dimensional data structure that has 18 columns correspond to each channel and a few thousands of rows that represent data instances collected over time by the BrainAmp amplifiers with 1000 samples per second. These data structures are called data sets which are a special type 2-dimensional data arrays.

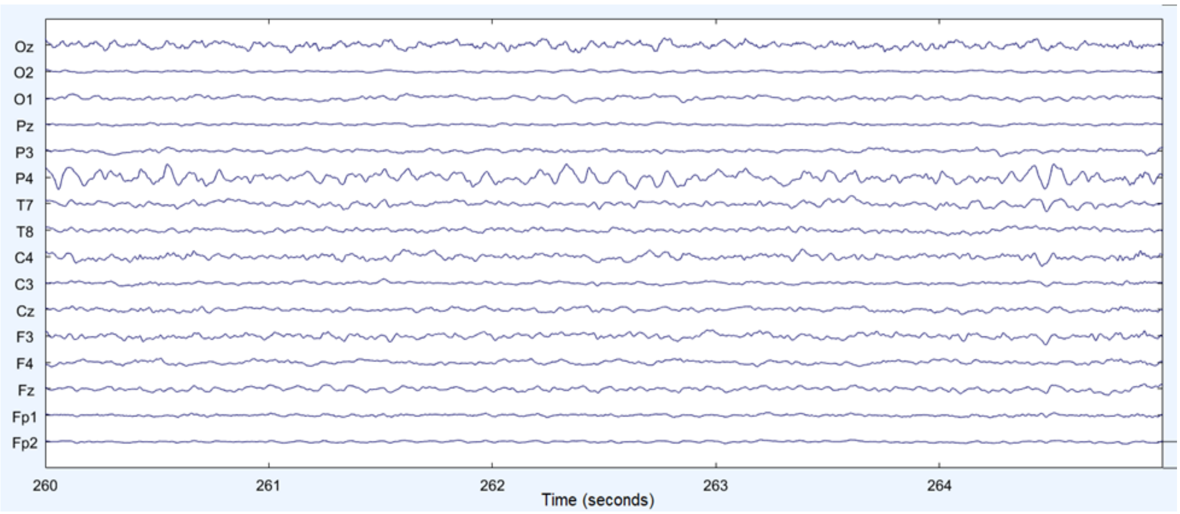

Figure 2.2: Sample 5 Seconds of Clean EEG Data.

2.3 CLASSIFICATION ALGORITHMS

Classification is the main step in the machine learning pipeline. It involves using one or more classification algorithm. A self-developed MATLAB routine was used to calculate the power of the different frequency spectrums of the EEG data. The data then was fed into several classification algorithms, namely K-Nearest Neighbour (K-NN), Decision-Tree (DT), Support Vector Machines (SVM), and Linear Discriminant Analysis (LDA) are discussed in the following sections.

2.3.1 Decision Tree (DT)

Decision trees are a type of supervised classification algorithms that divide the classification problem into a subset of less complex problems, a process which is repeated to the subsets as well until a multi-node tree is formed [67]. In a decision tree, each nonterminal node represents a test for a particular feature fed into the algorithm as the classification criterion, nodes resulting from other nodes (branches) are the results of such a test, whereas the terminal nodes hold a label for a feature class. An example of a decision tree is shown in figure 2.3 below. It supposes a customer prediction of being highly to buy or low to buy product from a proposed electronics market upon certain criterions. In this process, and in the root (first top) node of the tree, it will check whether customer age between 20-40, if not, he is low probable to buy. If so, then system check whether he has an active job, if not, then he is low probable to buy. If yes, then it is checked whether he receives a salary equal or more than 1000$, if no, then he is low probable to buy, but if yes then system checks whether he shown previously high interest in a certain group of products. If yes, then he is high probable to buy, if not then checks whether he had bought enough product or products within the last six months from the market. If yes, then he has high probability to buy, else, he shows low probability to buy.

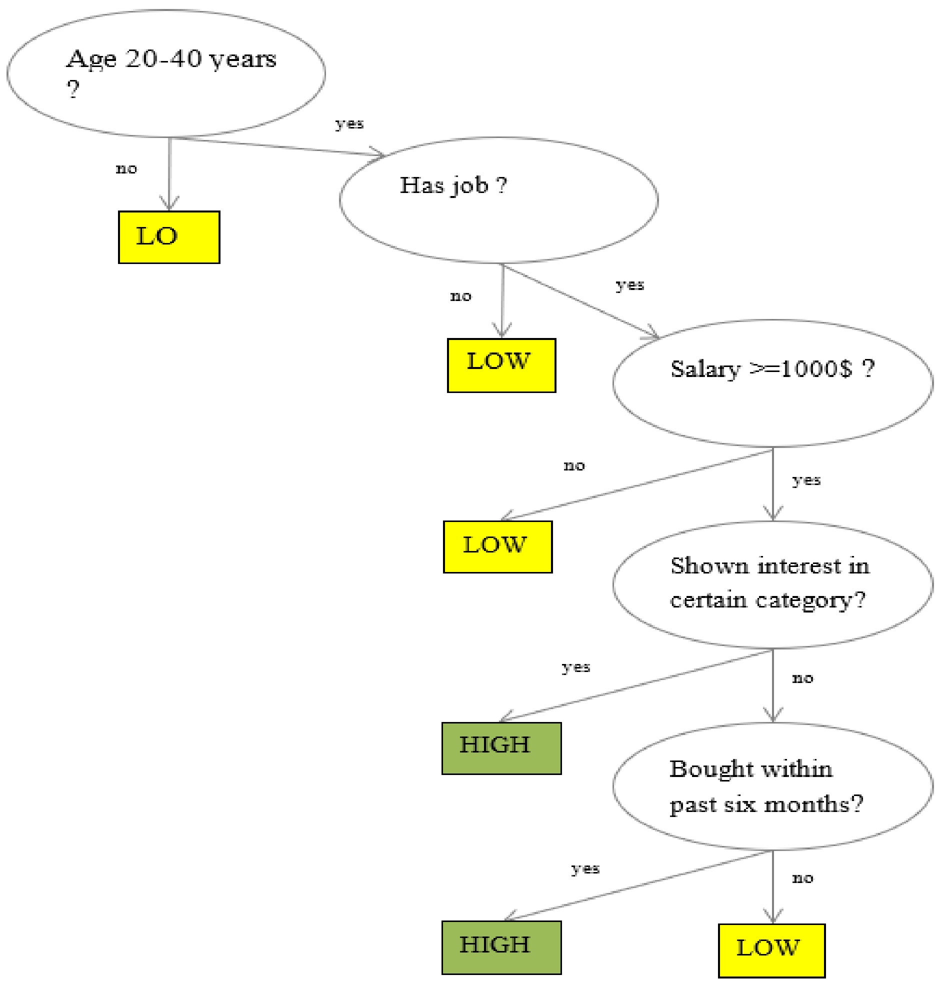

Figure 2.3: Decision Tree Construction to Predict Two Classes High Buy or Low Buy.

The process of creating subsets uses a metric function to evaluate the split resulting from the test nodes. Such metric functions include Gini index and information gain. Gini index measures the degree of impurity of the data, such that a Gini value of 0 represents complete purity, whereas a Gini value of 1 means completely impure. It is defined as the sum of the squares of the probabilities for a data element to belong to a class Ki., for all data values n, as shown in equation 2.1 below:

$$Gini(Dat) = 1 - \sum Pi^2 \quad (2.1)$$

Where Pi is the probability that a data sample in Dat belongs to a specific class Ki.

Information gain on the other hand is a feature selection tool that captures the degree of importance a classification attribute carries. In other words, it captures the attribute with the highest weight (gain) in determining the class of the data, thereby minimizing the amount of attributes needed for classification. Mathematically, it is defined as the negative products of the probability of a test data i to belong to a class Ki with the base 2 logarithm of that probability, summed across all data points, as shown in equation 2.2 below:

$$Info(Dat) = -\sum Pi\ log2(Pi) \quad (2.2)$$

Among the two attribute selection measures introduced above, Gini index is the measure that imposes a binary shaped tree, whereas using information gain does not necessarily produce two result nodes out of each test node.

The process of creating the appropriate decision tree classifier involves the step of induction, which is don through one of three well known algorithms, C4.5, ID3, or CART. This process creates a flow chart like a construction of steps within which internal and external nodes are created. In the classification task, any test of an attribute stands for an internal node creation, whereas the output of that test stands for a tree branch creation, while the result of class distinguishing stands for external node creation. For example, the process of constructing a decision tree using the C4.5 type algorithm can be shown below in figure 2.4.

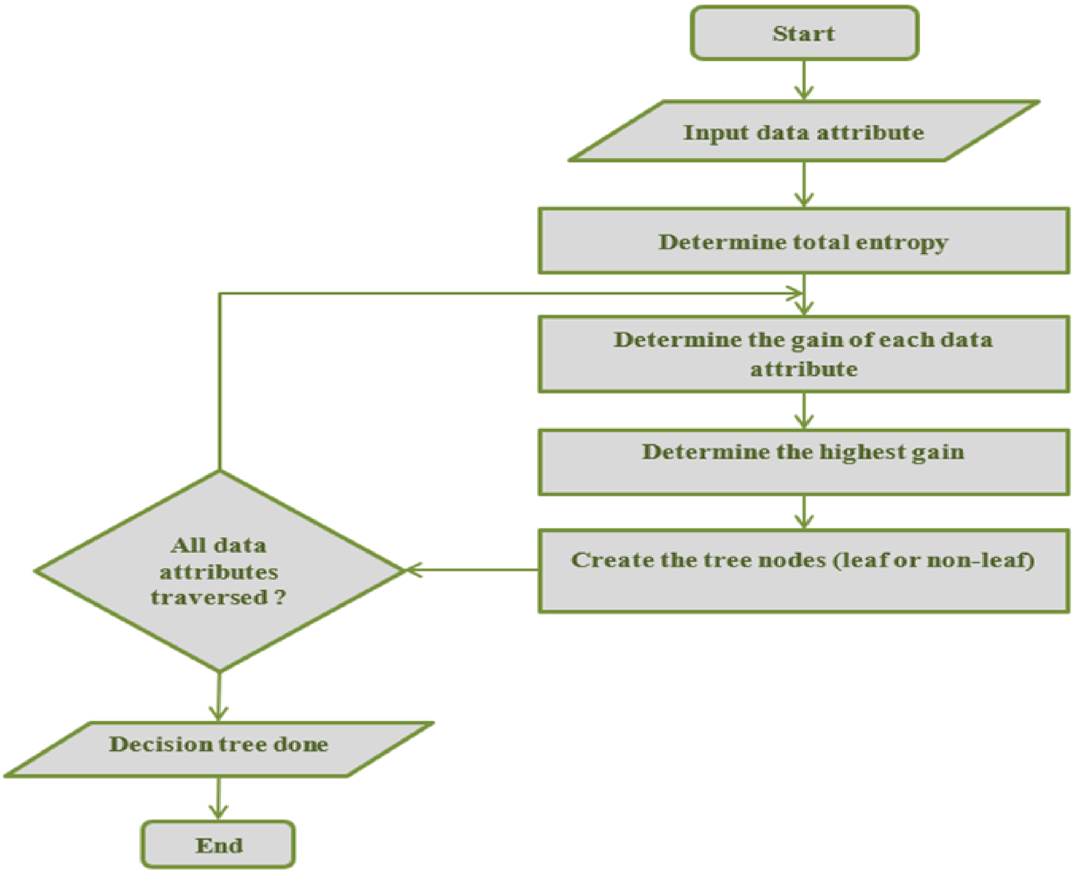

Figure 2.4: Construction Decision Tree Using C4.5 Algorithm.

2.3.2 K-Nearest Neighbour (K-NN)

In order to classify certain invisible data to the classifier to one particular class, K-Nearest Neighbour (K-NN) algorithm uses the neighbouring data points, K-number of neighbouring points, to assign a class to the unknown data point. The algorithm measures the difference between a data point and a K-number of neighbouring points surrounding it using distant metrics such as Euclidean distance given in equation 2.3, which defines the distance d that separates between two points k and l as below:

$$d_{k,l} = \sqrt{(d_{k1} - d_{l1})^2 + (d_{k2} - d_{l2})^2 + \cdots + (d_{km} - d_{lm})^2} \tag{2.3}$$

After distances are obtained, the data point is assigned to the class that has the greatest number of points among its neighbours and said to be belonging to that type or class.

2.3.3 Logistic Regression (LR)

In order to compare two or more explanatory (independent) variables in terms of their effect on a dependent variable, logistic regression is utilized [68]. Logistic regression is makes use of the odds ratio (OR), which represents the ratio between the odd of a dependent event to occur in case an independent event occurs and the odd of the same event to occur if the independent event does not occur [69]. Mathematically, OR is calculated as in equation 2.4 below:

$$OR = \frac{odds\ of\ the\ events\ in\ the\ dependent\ group}{odds\ of\ the\ events\ in\ the\ independent\ group} \tag{2.4}$$

In logistic regression, ORs are used to find the cofactors of the logistic regression's binomial, which relates the probability of an event to occur to each independent variable in the binomial as per equation 2.5

$$\log\left(\frac{\pi}{1-\pi}\right) = B_0 + B_1x_1 + B_2x_2 + \cdots B_mx_m \tag{2.5}$$

2.3.4 Linear Discriminant Analysis (LDA)

Linear discriminant analysis is a linear and supervised classification technique that aims to find a set of features (discriminant) that help with the process of differentiation between different classes. Using Bayesian probability theory, it estimates the output probability using the input and may be used as a dimension reduction technique. LDA projects features from lower dimensions to higher dimensions. The mathematical basis of Bayesian probability is utilized in LDA by using the probability of each class as well as the probability of a data element to belong to a certain class. Equation 6 shows the mathematical representation of the Bayesian probability theory:

$$\mathrm{P}(B|A) = \frac{\mathrm{P}(\mathbf{B} \cap \mathbf{A})}{\mathrm{P}(\mathbf{A})} = \frac{\mathrm{P}(A|B)\mathrm{P}(\mathrm{B})}{\mathrm{P}(\mathrm{A})} \tag{2.6}$$

Where P(B|A) is the posterior probability or conditional probability, which is the probability of B provided that A is true. P(B) is the initial probability of B, which is known as the prior, P(A) known as the likelihood.

2.3.5 Support Vector Machine (SVM)

Similar to LDA, Support Vector Machines (SVMs) transform information from lower dimensions to higher dimensions. This process is used using a nonlinear mapping algorithm. In the new dimension the points are separated into classes using a linear separation decision boundary which is found by searching for the optimal boundary that creates the largest distance possible between data point of different classes.

The number of features to be classified determines the dimensions of the boundary. A binary feature classification problem requires a 1-dimensional line as a boundary, whereas classifying three features requires a plane (2-dimensional) as a boundary. Classifying more than 3 features would require a multidimensional boundary: a hyper plane. As an example, first we define a classifier of a linear type as per equation 2.7:

$$f(x) = sign(z^T x + a) \tag{2.7}$$

where, z is a vector of N dimension and a is a scalar.

With the assumption of $f(x_k) = +1$ if $y_k = +1$ and $f(x_k) = -1$ if $y_k = -1$, when we take a signal x_k $(k = 1,2,3,\ldots,N)$ as an input and want to classify between two classes, $y_k = +1$ class for positives and a class labeled $y_k = -1$ for negatives. The best solution provided by SVM is to find the hyper plane that defines the maximum distance from the closest point in both positive and negative sides, which is known as the maximum margin as in figure 2.5.

To find that best hyper plane, we will assume a hyper plane ρ is defined through z and a being group of points such as in equation 2.8:

$$\rho_{z,a} = [x \mid z^T x + a] \tag{2.8}$$

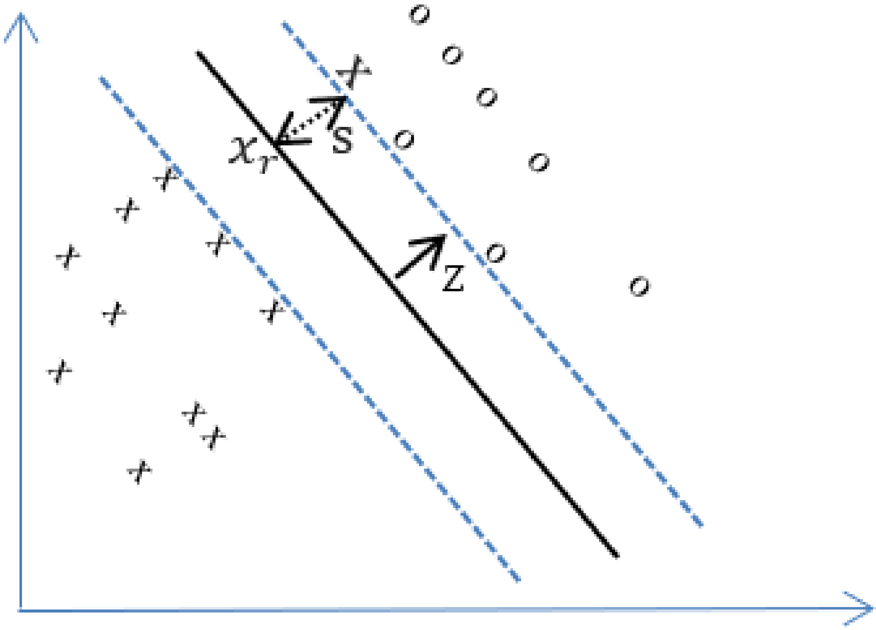

Figure 2.5: SVM Maximum Margin Construction.

Now, we have to define the margin s as to be the distance from any point X on both sides to the separating hyper plane ρ, then $x_r = x - s$ is the extension of the point x onto the hyper plane ρ.

Then distance s can be found such as $s = \alpha z$, as s is known to be parallel with z, for α ∊ R, and as $x_r \in \rho$ so we replace for x_r value and get equation 2.9 below:

$$z^T x_r + a = 0 \tag{2.9}$$

Plugging the definitions of x_r and s into the previous equation will lead to find value of α as equation 2.10 below:

$$\alpha = \frac{z^T x + a}{z^T z} \tag{2.10}$$

Finally, the distance s is found as in equation 2.11:

$$s = \frac{z^T x + a}{z^T z} z \tag{2.11}$$

2.4 PERFORMANCE MEASURE METRICS

Measuring the performance of our study findings is a step towards interpreting the research findings as well as objectively evaluating the research work done. Such measurement makes use of several statistical metrics, some of which will be discussed in the next sections. These metrics directly or indirectly use the number of true positives (TP), false positives (FP), true negative (TN) and false negatives (FN) which are representing the classification model results after applying the required input data samples. TP samples are denoting the positive values from the test part of the input data that were correctly classified by the model, the FP on the other hand denotes the positive values were wrongly classified using the model, whereas the TN denotes the negative of test data values of which were classified correctly, where FN denotes the negative values which were falsely classified. The following confusion matrix which represents a two classes problem and include all the previous concepts is shown in Table 2.1 below:

Table 2.1: Confusion Matrix of Two Classes Problem.

		Predictions	
		Class 1	Class 2
Actuals	Class 1	TP	FN
	Class 2	FP	TN

2.4.1 Accuracy

The classification model accuracy is the percentage of the test data set samples which were predicted to be one of the classes correctly. The accuracy is defined such as in equation 2.12 below:

$$Accuracy = \frac{TP + TN}{TP + TN + FP + FN} \qquad (2.12)$$

2.4.2 Sensitivity

Sensitivity is measured as the ratio between the true positive (TP) and the sum of true positive and false negative (TP + FN), thereby represents the possibility of getting a positive result. Mathematically, it is expressed as shown in equation 2.13 below:

$$Sensitivity = \frac{TP}{TP + FN} \tag{2.13}$$

2.4.3 Specificity

Specificity is complementary to sensitivity. It measures the possibility of getting a negative outcome by taking the ratio between the true negatives and the sum of both true negatives and false positives. The mathematical expression of specificity is shown in equation 2.14 below:

$$Specificity = \frac{TN}{TN + FP} \tag{2.14}$$

2.4.4 Precision

Precision, or confidence, is the ration between true positives and all positives (true and false). It is a direct estimation of the ability of the test to properly identify the positive cases. Mathematically, precision is given as per the equation 2.15 below:

$$Precision = \frac{TP}{TP + FP} \tag{2.15}$$

2.4.5 ROC Curves

Receiver operator characteristics (ROC) curves are curves constructed by plotting the specificity of a test on the x-axis and its sensitivity on the y-axis. Such curves show the discriminative capability of the test and are also required for calculating the area under ROC curve (AUC). The closer the ROC curve is located to the top-left corner the better the discriminative ability of the test is [70]. Figure 2.6 shows an example of plotting ROC curve for a proposed classifier.

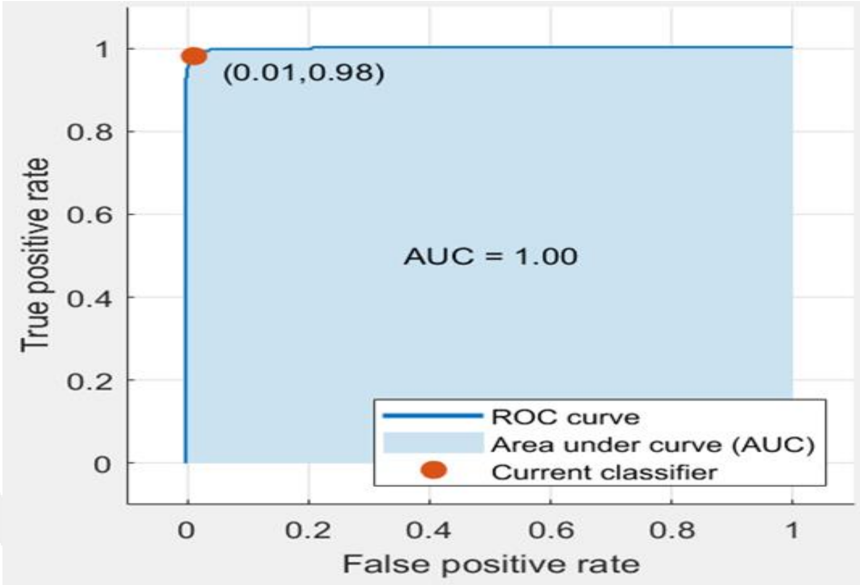

Figure 2.6: ROC Curve for SVM Classifier.

2.4.6 F1-Score

F1-Score represents the combination that gathers both recall and precision in one graph and shows the balance between them. It is one measure that gives a good visual insight about classifier performance. F1-Score is defined in equation 2.16 below:

$$F1 - Score = \frac{2 * TP}{2 * TP + FP + FN} \tag{2.16}$$

2.5 EEG FEATURE SET

EEG signals are time-series signals composed of several frequencies. As a biological signal of high non-linearity, frequency analysis of EEG provides an easier insight to the signal. The Power Spectral Density (PSD) is used to obtain information regarding the different frequency bands, therefore the spectral power of each band can be used in classification algorithms as a feature. On the other hand, time series analysis of EEG signal is achievable through using one of the several types of entropy. The different entropy types may therefore be features of interest during classification. The above-mentioned features are considered among the set of calculated features used as input to the classification process which also include wavelet decomposition and statistical measures of the signal. It should be mentioned that calculated features are not the only type of features used for classification, since EEG generated spectrogram images and EEG signal strength are also used in classification [17].

These two sets of features have been used as a comparison parameter to study the ability of our suggested system to differentiate between different subject physical tiredness states reflected by the lactate enzyme blood levels. The EEG frequency Band Power (BP) feature was the first set to be extracted, studied and reported in a published research paper[71], while Sample Entropy (SaEn) was the second feature extraction method in our study. The following sections show the employment of both BP and SaEn into the classification algorithms was achieved.

2.5.1 Three Classes Applied Features

To find whether we can use our system to identify not only between two classes, high-lactate and low-lactate that reflect the physical tiredness status of the subject respectively, but also three classes lactate-level-high, lactate-level-mid, and lactate-level-low. we brought the desired data set and applied required feature extraction methods that most fits with our intended goal. Besides the BP feature mentioned in the previous section, SaEn as a measure of uncertainty that was extracted and employed offering the opportunity to utilize it as a classification feature revealing the time series information carried by the EEG signal. It represents a statistical measure for the time series signal complexity. The formula used to calculate SaEn is detailed in section 1.7. Sample entropy provides advantages over some other types of entropy particularly approximate entropy as previously discussed. It eliminates self-matching, more consistent and less dependent on data length. Sample data from both BP and SaEn feature sets are shown in figures 2.7 and 2.8 respectively.

CH1					CH2					CH16					Class
Delta	Theta	Alpha	Beta	Gamma	Delta	Theta	Alpha	Beta	Gamma	Delta	Theta	Alpha	Beta	Gamma	
80.84741	19.67441	60.23568	82.81004	74.26293	8.990271	6.720795	8.946677	32.19973	21.98189	21.34291	7.193708	10.72207	32.9541	26.92057	1
53.3764	19.89426	32.4834	60.01958	39.66953	23.57482	8.486279	14.15417	32.71905	25.08954	22.3985	6.169715	12.25657	32.33102	24.34103	1
67.71618	33.58978	51.94473	66.85143	36.49279	18.30618	8.971986	7.989719	34.32887	24.00437	6.958208	7.958621	8.448857	26.95144	15.47906	1
59.08141	11.24495	53.27552	69.80237	41.26717	68.78925	16.95186	16.13077	26.89492	24.15552	65.37435	17.28944	11.77873	26.73208	27.01412	1
59.73356	22.00466	46.66506	81.60209	48.13332	13.99071	4.599065	9.007098	33.32604	24.63182	14.16246	5.371491	7.480762	39.83542	22.65007	1
28.87491	34.0835	23.69091	93.66359	47.70363	19.78504	7.335328	7.445432	36.71297	21.62977	18.76383	7.300424	8.361764	31.25857	22.24699	1
78.84018	24.04579	51.76187	88.34744	58.84338	17.23057	9.82107	11.28146	36.7221	17.25649	10.72732	6.577231	9.522	32.07436	22.66132	2
60.17191	28.15208	40.14324	63.73481	43.46685	17.66992	5.086454	8.856805	30.75676	21.73999	18.57852	5.512261	7.715701	32.0304	17.90254	2
43.52	19.94579	30.69003	62.49186	28.20888	8.348691	7.165625	5.942059	28.35472	18.49786	9.009136	7.020394	5.850102	27.61918	17.23028	2
88.26508	25.43481	46.21482	61.58935	36.8164	88.44535	21.1193	14.021	33.18886	22.14325	60.01557	15.78323	11.50282	33.3538	18.48745	2
91.70961	16.86215	43.9024	66.34342	30.93226	7.733835	7.002028	8.280673	33.56905	23.81771	21.33735	8.265021	11.74039	30.29392	18.80233	2
55.92057	23.69998	42.24322	51.2221	37.86069	13.43701	5.858977	12.28602	40.93842	21.97036	6.438357	5.171063	8.287182	34.95508	23.78117	2
58.13352	31.4662	43.33821	53.74114	34.43407	15.73654	3.897881	11.49895	34.83296	17.87204	15.69927	7.059302	9.931808	31.2664	21.36562	3
34.1357	18.69089	37.23475	65.40084	37.65481	15.05116	8.616147	16.05319	36.61954	20.38595	17.44939	6.377049	18.84361	26.8139	23.02375	3
125.5128	26.13338	40.46784	144.2285	110.4597	13.35338	4.731876	17.49294	33.78757	22.81672	16.77577	6.190049	17.35394	30.97485	18.07177	3
89.71388	33.20117	42.24944	64.69664	34.67451	7.650447	4.624064	11.52489	31.21696	20.23195	15.54402	6.794287	11.79206	32.07925	20.76317	3

Figure 2.7: Three Classes BP Feature Sample.

CH1	CH2	CH3	CH4	CH5	CH6	CH7	CH8	CH9	CH10	CH11	CH12	CH13	CH14	CH15	CH16	Class
1.1458	0.40281	0.57183	0.34315	0.6025	0.40325	0.79398	0.63876	0.64036	0.76737	0.76606	0.49993	0.78699	0.79798	0.57336	0.55684	1
1.15016	0.28893	0.56879	0.3946	0.6197	0.44031	0.46772	0.70789	0.57334	0.77652	0.72489	0.50254	0.70397	0.60746	0.53031	0.56072	1
1.07938	0.4375	0.61456	0.34351	0.542	0.40655	0.76316	0.68849	0.63376	0.73494	0.7643	0.41342	0.69775	0.7938	0.53317	0.54502	1
1.14547	0.14816	0.62108	0.38818	0.66141	0.37336	0.41681	0.73335	0.53338	0.7228	0.70233	0.37437	0.71342	0.64658	0.59565	0.5719	1
1.12458	0.16648	0.60858	0.345	0.57413	0.39784	0.44866	0.67586	0.55013	0.76775	0.50835	0.52687	0.77219	0.70098	0.48387	0.42729	1
1.28395	0.30402	0.53467	0.27507	0.50147	0.45573	0.49334	0.6124	0.64787	0.76193	0.78679	0.34346	0.73114	0.71454	0.49961	0.5682	1
1.1598	0.38854	0.5525	0.33615	0.59179	0.46823	0.41534	0.65297	0.58366	0.7708	0.77883	0.28575	0.69784	0.67149	0.52063	0.57649	1
1.27688	0.42757	0.63077	0.36027	0.59596	0.44842	0.68021	0.65562	0.46465	0.76653	0.77669	0.44106	0.7327	0.70732	0.48609	0.56691	2
1.18878	0.18897	0.56328	0.44576	0.47599	0.4556	0.58527	0.65677	0.59921	0.79488	0.82442	0.40929	0.75801	0.75329	0.57115	0.49423	2
1.29007	0.42232	0.55999	0.41748	0.56426	0.43255	0.45197	0.62596	0.56534	0.75716	0.65991	0.25454	0.60023	0.64263	0.47553	0.51377	2
1.22126	0.23619	0.42919	0.34438	0.53662	0.37277	0.60307	0.60075	0.68846	0.76278	0.73294	0.29231	0.64239	0.7068	0.36789	0.54409	2
1.29668	0.22017	0.31759	0.38211	0.48844	0.5139	0.65221	0.6084	0.62605	0.71456	0.73014	0.36787	0.65697	0.55091	0.41903	0.51314	2
1.28425	0.18546	0.55865	0.42253	0.55521	0.50261	0.73017	0.6039	0.64636	0.78917	0.81847	0.50615	0.77048	0.58094	0.53024	0.48865	2
1.30194	0.42282	0.64072	0.34031	0.57451	0.48573	0.78392	0.57874	0.5881	0.75703	0.63401	0.46283	0.60379	0.58586	0.5377	0.56409	2
1.27488	0.3568	0.46156	0.34949	0.53478	0.43849	0.73997	0.5166	0.52626	0.78621	0.62361	0.4721	0.60142	0.46332	0.54869	0.48542	3
1.21516	0.43179	0.58619	0.36847	0.53363	0.52284	0.77844	0.66202	0.63703	0.79167	0.76073	0.41363	0.73588	0.41401	0.55246	0.57296	3
1.24867	0.22695	0.5502	0.32842	0.57793	0.40535	0.66751	0.63158	0.58191	0.78607	0.74901	0.38108	0.72711	0.46306	0.51557	0.52611	3
1.21358	0.19322	0.5251	0.33283	0.51393	0.37337	0.72721	0.59032	0.43258	0.79385	0.61536	0.21629	0.77575	0.62267	0.56733	0.56133	3
1.25585	0.22096	0.62481	0.34244	0.59533	0.48419	0.77299	0.60839	0.66895	0.74526	0.78863	0.42529	0.78432	0.59775	0.54471	0.52748	3
1.25756	0.2631	0.64544	0.42963	0.496	0.50054	0.80158	0.60831	0.63772	0.79058	0.74908	0.21323	0.76382	0.70845	0.58574	0.51006	3

Figure 2.8: Three Classes SaEn Feature Sample.

2.5.2 Two Classes Applied Features

EEG signals are known to include valuable information in its frequency domain. The Power Spectral Density (PSD) of the EEG signal provides information about the power of each frequency band, which is associated with different types of physiological and psychological activities [72]. By utilizing the band power feature of the EEG signal which is a non-stationary time-series sequence, the power spectral density PSD describes the energy distribution of the EEG bands intensity [73]. As previously mentioned in section 1.6, FFT is used to obtain the frequency information and therefore powers of different frequency bands from the EEG recordings. It provides the frequency representation for the EEG bands, namely Delta, Theta, Alpha, Beta and Gamma in the frequency domain. It divides the input signal into equally spaced samples and outputs the frequency spectrum according to equation 2.17 below:

$$X(f) = \int_{-\infty}^{\infty} x(t)e^{w}dt \tag{2.17}$$

Where $X(f)$ is the output in frequency domain, $x(t)$ is the input in time domain, w is the complex exponent that equals to $2\pi jft$, where f is the frequency and t is the time. Band power has been found to offer promising results in several BCI applications, particularly for those intended for the emotion recognition [74].

With this feature set, and after applying suitable data pre-processing and artefact removal techniques that led to a clean EEG data set, we used a MATLAB routine to extract the intended data feature set that represent low-lactate and high-lactate within the two stages, pre-exercise and post-exercise. These feature sets then combined in a form of data structure called dataset. It is a 2-dimensional data array of 7759X80 dimension. The first number (7759) denotes the count of data samples collected over time, within each one contains details about the BP feature for all the 16 channels. Each channel with five band contains a feature then 16 multiplied by 5 leads to 80 features. On the other hand, the last column in the feature set will represent low-lactate before exercise denoted by digit "1" in the file, while digit "2" denotes high-lactate after exercise.

2.6 LACTATE DEHYDROGENASE ENZYME (LDE)

Lactate Dehydrogenase Enzyme (LDE) is an enzyme that enhances the transformation of pyruvate, which generated from the glycolysis of glucose in the body [75], into lactate as well as converting nicotinamide adenine dinucleotide (NAD)H to NAD+. This process naturally occurs during generation of the adenosine triphosphate (ATP), which is considered the fuel of the cells. The generation of LDE and its usage as an indicator for fatigue is discussed in the following sections.

2.6.1 Glycolysis and Lactate Dehydrogenase Enzyme

Generation of energy in the human cells -and in other creatures in general- is a multi-phased process involving the conversion of glucose into energy (particularly into adenosine triphosphate or ATP) through aerobic combustion. The process in conditions where glucose is abundant involves converting pyruvate generated from glycolysis into acetyl-CoA, which in turn is used to fuel the formation of ATP through oxidation. ATP generation using glycolysis involves converting glyceraldehyde 3-phosphate (GADP) to D-1,3-bisphosphoglycerate (1,3BPG) using nicotinamide adenine dinucleotide (NAD+). Since NAD+ is formed through an oxidation process, situations where oxygen levels are low obstruct NAD+ production. This in turn is a signal to start using anaerobic glycolysis as a main source for ATP generation. During anaerobic glycolysis, LDH helps NAD+ production to take place without the presence of oxygen by converting NADH into NAD+ and lactate is generated as a by-product [76].

Since LDH is produced during hypoxic situations in the cell, it can be used as an indicator of the severity of exercise and degree of exhaustion. LDH level is measured through various samples taken from the subject, including serum, plasma, tissue, and cell samples. Care is required when taking the measurements from serum and plasma as erythrocytes in the blood may release LDH on rupture, thereby showing a false increase.

2.6.2 Evaluation of Lactate Dehydrogenase Enzyme

The lactate dehydrogenase enzyme measurements which have been done along the experimental steps was reported and found to have an increase pattern from the start until the end of exercise sessions, and after a period of rest it starts to decrease going again to be near from the first measures but with a slower pace compared to its first increase pace. Within the first 2 minutes, it was reported to have values ranging between 1 - 4 millimol/L, and in the second 2 minutes it was ranging between 2 - 6 millimol/L and so on until it reaches the highest range between 4 - 14 millimol/L within the period from 8^{th} minute up to 10^{th} minute. These measures were reported in the period of rest following the completion of exercise session after the 10th minute as follows, they ranged between 3.5 - 13.5 millimol/L within 12^{th} and 14^{th} minutes, while found between 2.5 - 13 millimol/L within minutes 16^{th} and 18^{th}.

These measurements infers the fact that the lactate dehydrogenate enzyme has a tendency to increase significantly affected by the sessions of acute exercise and maintain its high levels in the blood for an obvious period of time of many minutes, while it starts to decrease derived by a multiple minutes period of rest but with a slower pace compared to its increase pace which makes it a desirable indicator of physical tiredness level to be studied and utilized together with the EEG signal recordings, in contrast with other factors that can affect and cause an increase in the enzyme levels like fear or mental disruptions, within which the lactate enzyme takes further time to decrease and go back to its original state. These measures where used to evaluate the results and findings of our study that illustrates the rising levels of lactate enzyme impacted by acute exercise sessions, which were reflected by the differences observed on some features of EEG signal. These findings were verified and found to be in agree with the reported values of lactate enzyme levels, low before exercise, moderate during exercise and high after exercise.

2.7 PHYSICAL TIREDNESS CLASSIFICATION SYSTEM (PTCS)

Our study focus was to build a machine learning based system that takes EEG recordings as an input and use them as a factor to discriminant different physical tiredness status of human body. The system was proposed to consist of multiple steps as follows in figure 2.9. The first system step involves using the collected EEG signals from the subjects while they are in a resting state and sitting in a calm fashion on resting chair for multiple minutes. Then they are asked to do a simple test of backward digit spanning. The recording of EEG signals was made with 1 KHz sampling rate using the BrainAmp ExG amplifier and a 16 channels scalp helmet with dry nodes. The environmental condition of recording assured by having it take place in a dark room with lights off and occupied with sound and light isolation to prevent any disruption to the recorded signals. The next step involves taking the raw EEG data recorded in a specialized form of different size file that reflects how time series signals are filled with information along with many contamination artefacts. This makes the demand to use suitable signal pre-processing techniques to get a clean version of recorded data and make it applicable and usable for the next experimental steps. These techniques involved removing extreme data signals that exceeds the 100μV boundary in value. Furthermore, the low-pass filter was applied to exclude the data parts and make use of the useful EEG five bands, Delta, Theta, Alpha, Beta and Gamma which do not exceed 50 Hz boundary in frequency and crop any frequency above that. To get different components of EEG frequency bands separated from each other, a specialized decomposition routine has been developed and applied with the help of MATLAB application which gave us opportunity to make data ready for the rest steps of the experiment.

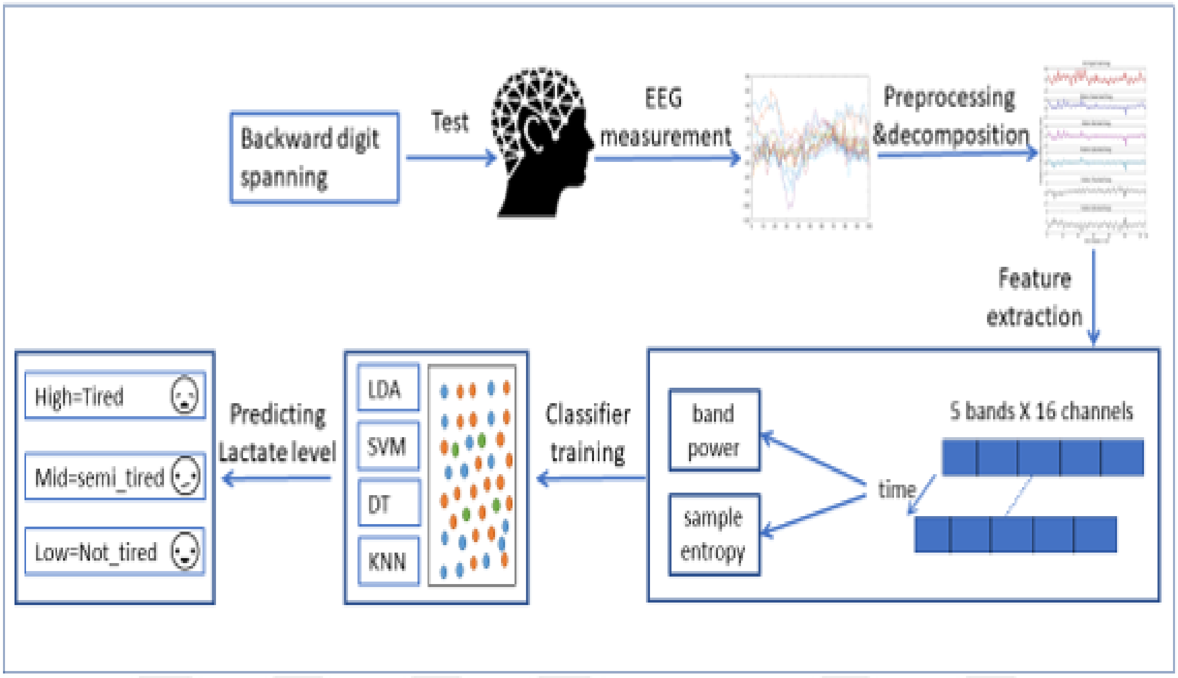

Figure 2.9: Physical Tiredness Classification System PTCS.

3. EXPERIMENTAL RESULTS AND DISCUSSION

3.1 EXPERIMENTAL RESULTS

In the context of results gained from our experimental steps through the study, we will divide them into two stages, first one involves results related with two classes prediction, and the other with the three classes prediction tasks as explained in the next sub-sections.

3.1.1 Two Classes Feature Results

In this part of thesis, we discussed the use of only two classes from that data, while all the three classes will be discussed in the next section of this thesis. We applied the following three classifiers: K-NN, DT and LR, to examine the performance measure over this dataset in terms of, accuracy, sensitivity, specificity, precision. These classifiers were discussed in section (2.3), while the performance metrics were discussed in section (2.4). The steps of our experimental work involve training the classification models with 80/20 train-test split ratio, that is 80% of data is considered for training the classifiers, while considering the rest of 20% as a testing data. The K-fold cross validation is used with K=5 folds to evaluate and assess accurately the performance of the classifiers when applied against the test data portion. A self-developed code which has been written using Matlab programming language that offers required functionality for the proposed model, was used to achieve the results. A sample of the two classes band power feature set is shown in figure 3.1 below:

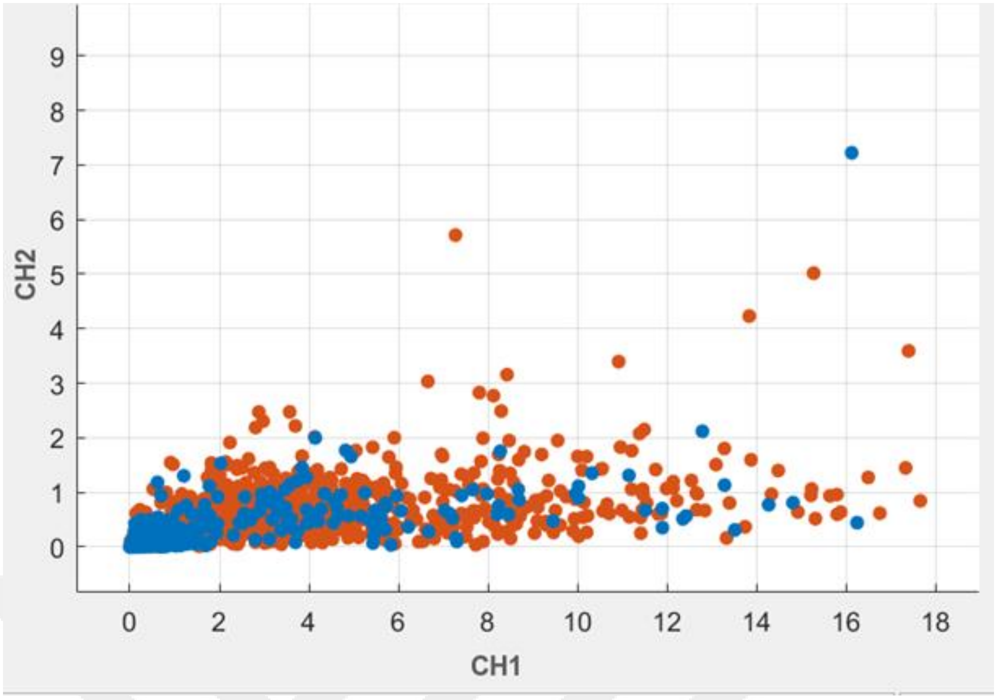

Figure 3.1: Sample of Two Classes Band Power Feature Set.

3.1.1.1 Accuracy results

Using the extracted band power feature and feeding them as an input to the classification models, using the Matlab imbedded machine learning application, showed a significant enhancement in terms of accuracy score of the classifiers. These finding results are listed in Table 3.1 below:

Table 3.1: Different Classifiers Accuracy Scores.

Classifier	LDA	LR	DT	K-NN
Accuracy%	50.5	70.0	98.0	98.4

The predictions of all the classification models, DT, K-NN and LR are shown in figures 3.2, 3.3, and 3.4 respectively.

As can be seen by the results listed in Table 3.1, the classification result for K-NN have been reported scoring best than other classifiers with 98.4%, followed by the DT and K-NN classifiers which had scored 98.0% and 70.0% respectively. Another classification model has been applied but showed a relatively low accuracy scores, LDA with 50.5%. This can be related to the data nature with which, a linear model like LDA that lacks the ability to find a good balance between the bias and variance to fit best with data and give the desired accuracy score results.

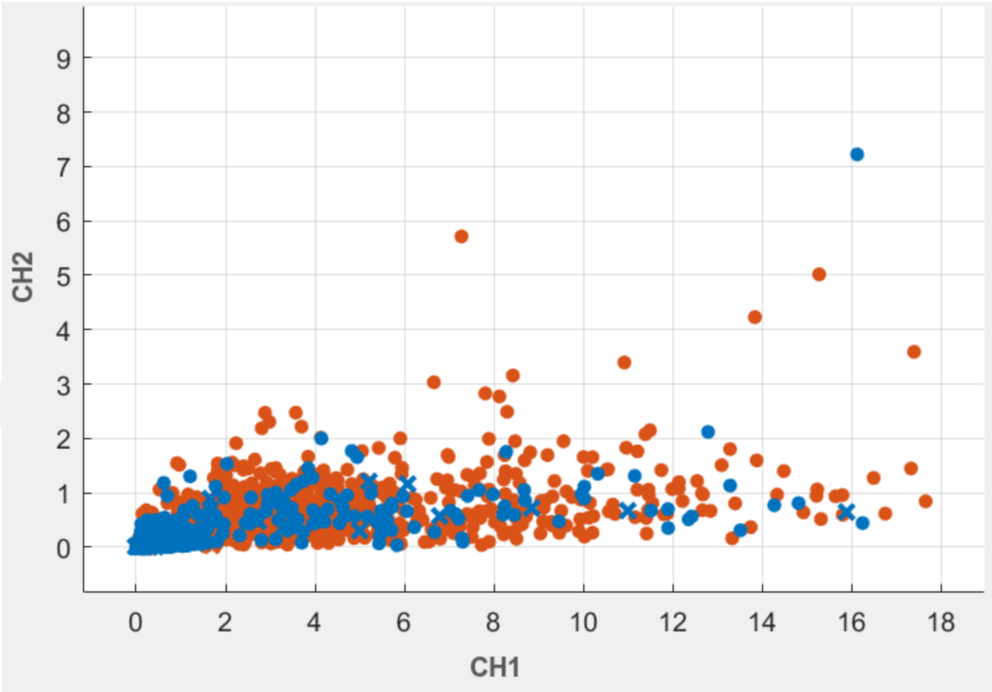

Figure 3.2: DT Model Predictions.

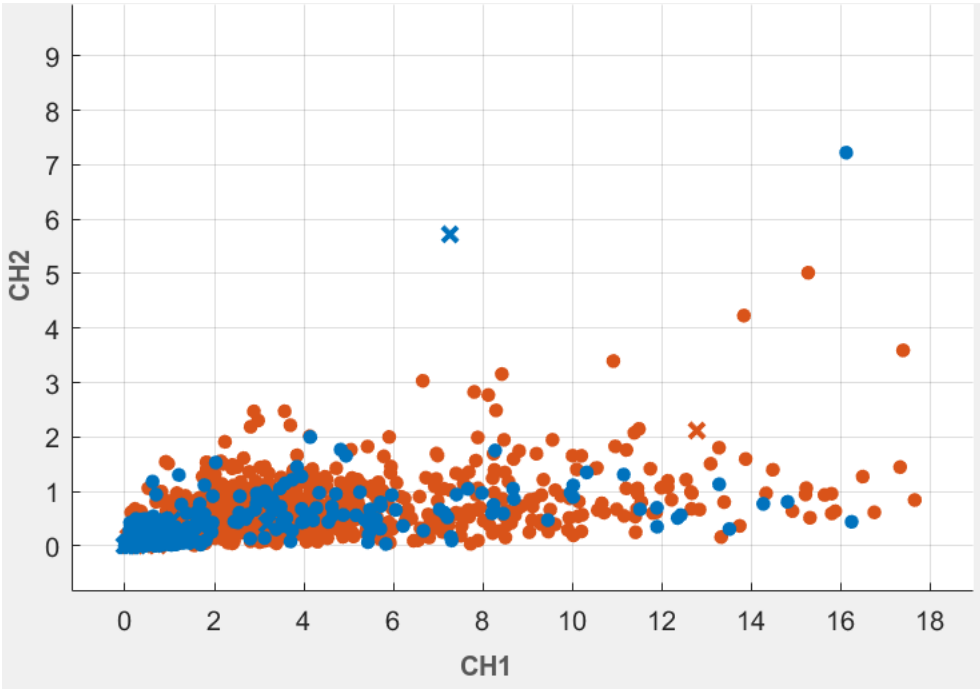

Figure 3.3: K-NN Model Predictions.

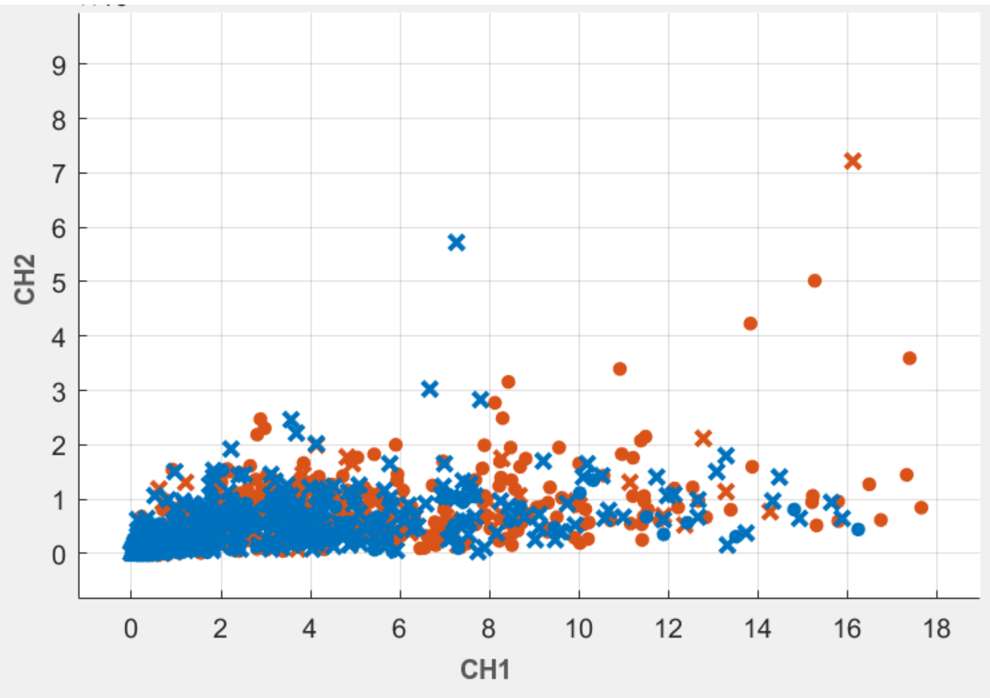

Figure 3.4: LR Model Predictions.

The above observations infer the high ability of the proposed system of feature extraction and selection by applying FFT to the EEG resting state data identifying the different physical tiredness states which is reflected by two classes, lactate-level-high and lactate-level-low. These findings show what we assume the best results in this field in the literature when utilizing machine learning techniques to investigate the athletes fatigue state before and after doing a single bout of an acute exercise session.

3.1.1.2 Sensitivity and precision results

Along with accuracy, we have used another two measures to clarify more precisely which classification model is better, these were sensitivity and specificity. As shown in Table 3.2, sensitivity and specificity results show that K-NN model had scored better for identifying true values of both classes, followed by the DT model and lastly the LR model. These results give the good impression about using K-NN as a good model with a high ability for correctly predicting true positive values (lactate-level-low) rate, as well as for correctly predicting true negative values(lactate-level-high) rate, that is the specificity measure. In contrast to K-NN and DT, the LR model had shown lower rates for predicting true positive and true negative rates.

Table 3.2: Different Classifiers Sensitivity and Specificity Scores.

Classifier	**LR**	**DT**	**K-NN**
Sensitivity%	76.5	97.2	98.8
Specificity%	64.0	94.2	97.0

Precision on the other hand tells us about the percentage of the lactate-level-low values that were predicted correctly and they we truly like so. The K-NN again over scores models as in Table 3.3:

Table 3.3: Different Classifiers Precision Values Distribution.

Classifier		Total	3867	3893	7760
K-NN	Actual class	Low-level-lactate	3790	76	3866
		High-level-lactate	77	3817	3894
			Low-level-lactate	High-level-lactate	Total
Predicted class					
		Total	3867	3893	7760
DT	Actual class	Low-level-lactate	3790	76	3866
		High-level-lactate	77	3817	3894
			Low-level-lactate	High-level-lactate	Total
Predicted class					
		Total	3867	3893	7760
LR	Actual class	Low-level-lactate	3790	76	3866
		High-level-lactate	77	3817	3894
			Low-level-lactate	High-level-lactate	Total
Predicted class					

3.1.2 Three Classes Feature Results

3.1.2.1 Band power sample features visualization

As our proposed model had used the band power feature extraction method to extract best discriminant criterion that distinguishes between two classes of the used dataset in the first experimental stage, here we had used the same method, but this time with three classes of the used dataset. The goal set for this stage is to find whether the band power feature will act well to discriminate between lactate-level-high, lactate-level-mid and lactate-level-low cases which reflects the three types of athlete's physical tiredness states, namely tired, semi-tired and very-tired encountered and reflected by the levels of lactate enzyme measures in the blood after performing a single bout of an acute exercise session. Firstly, in figure 3.5, it shows a sample from the three classes dataset and how it is distributed visually when plotted by using the plot function included in the Classification learner application in Matlab tool.

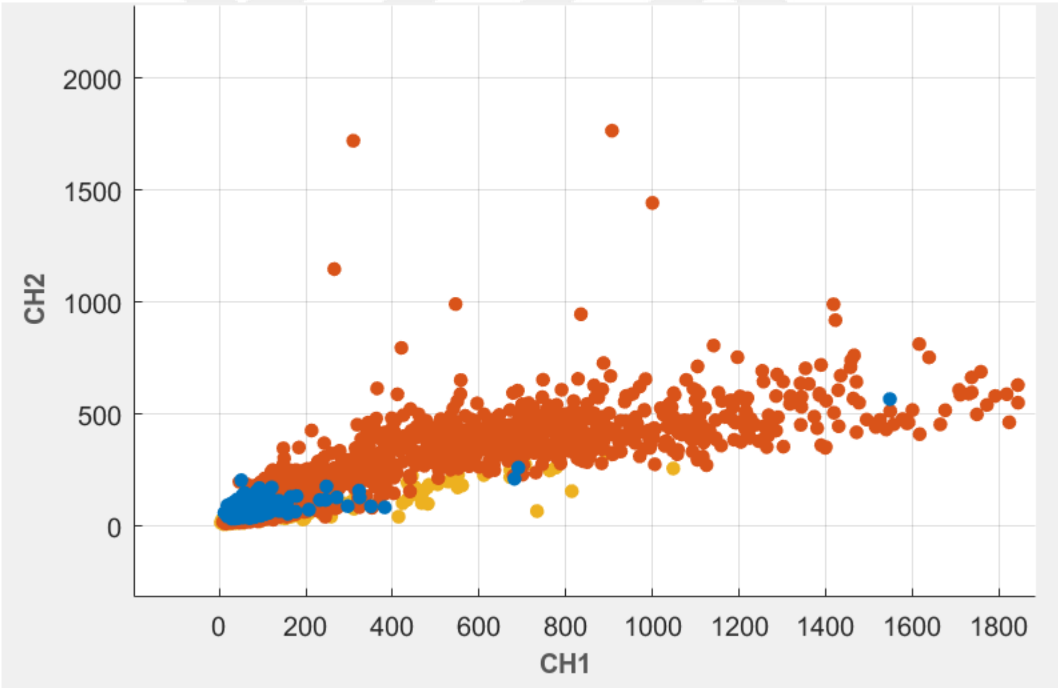

Figure 3.5: Sample of Three Classes Band Power Feature Set.

In this stage, we applied the DT, LDA, K-NN, and SVM classifiers to examine the performance measure against this dataset in terms of accuracy, precision, recall and F1-score.The same procedure which was applied with two classes, experimental work in this stage involved using the same train-test split ratio of 80/20 to use the majority of the dataset instances as a classifier model train data (80 %), while using 20 % to test the classifier ability to discriminate and correctly classify the unseen data instances in the same dataset, or even against a foreign EEG dataset. The proposed model performance assessment step, and for comparison reasons was performed using two different K-fold-cross-validator values, firstly with K=5 and later with K=10 folds applied against the results of classifier models result. We had used the same Matlab code machine learning app as with two classes to extract, select and feed feature set data to the model. Using the band power feature gave us the good model score results we were waiting for in terms of accuracy, precision, recall and F1-score with variations between applied classifiers. These classifiers with their predictions for all the DT, K-NN, LDA and SVM models can be viewed in figures 3.6, 3.7, 3.8, and 3.9 respectively.

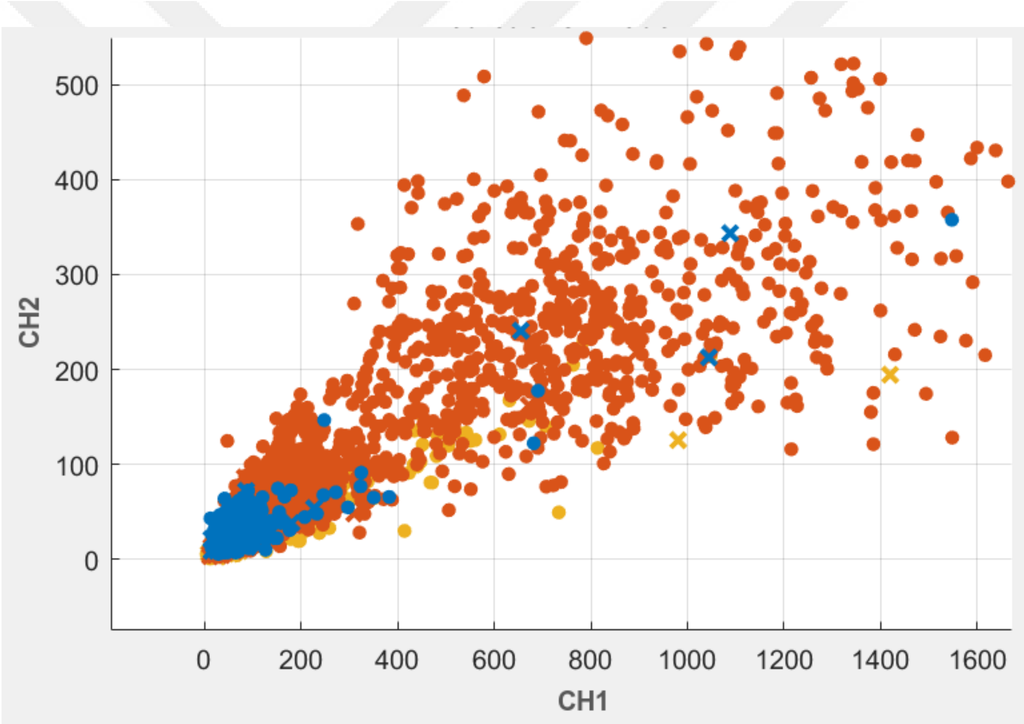

Figure 3.6: DT Model Predictions of Band Power with Three Classes.

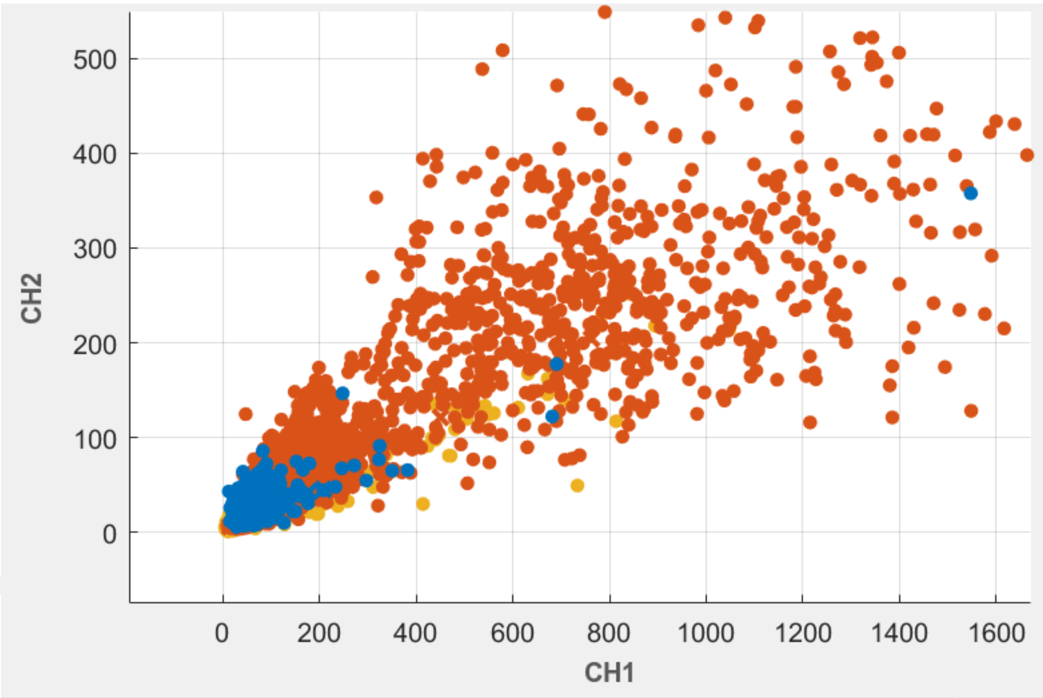

Figure 3.7: K-NN Model Predictions of Band Power with Three Classes.

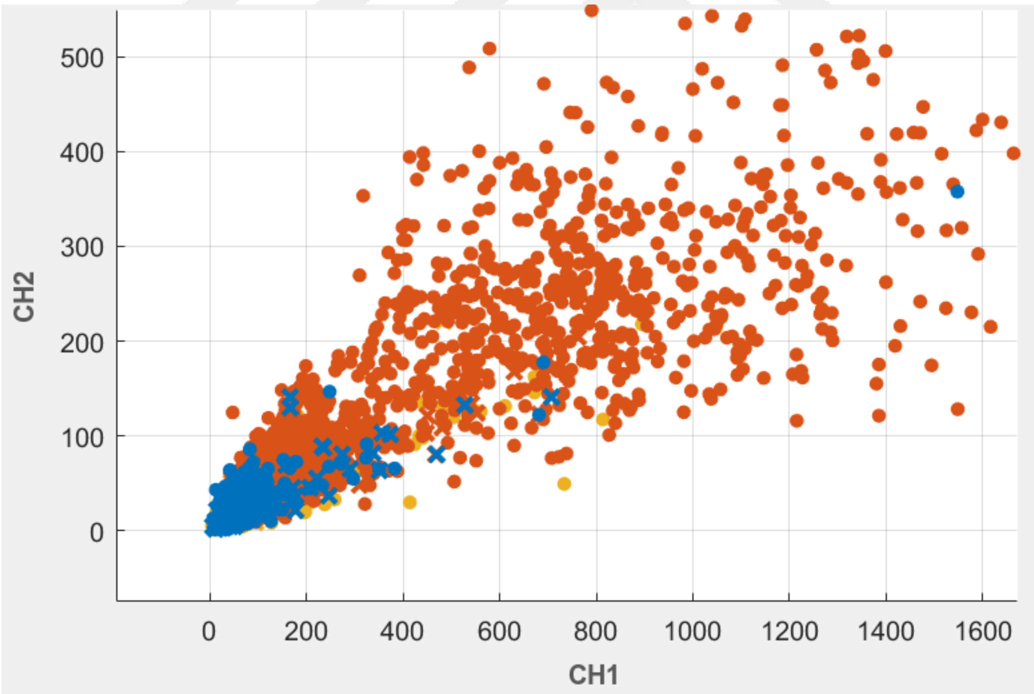

Figure 3.8: LDA Model Predictions of Band Power with Three Classes.

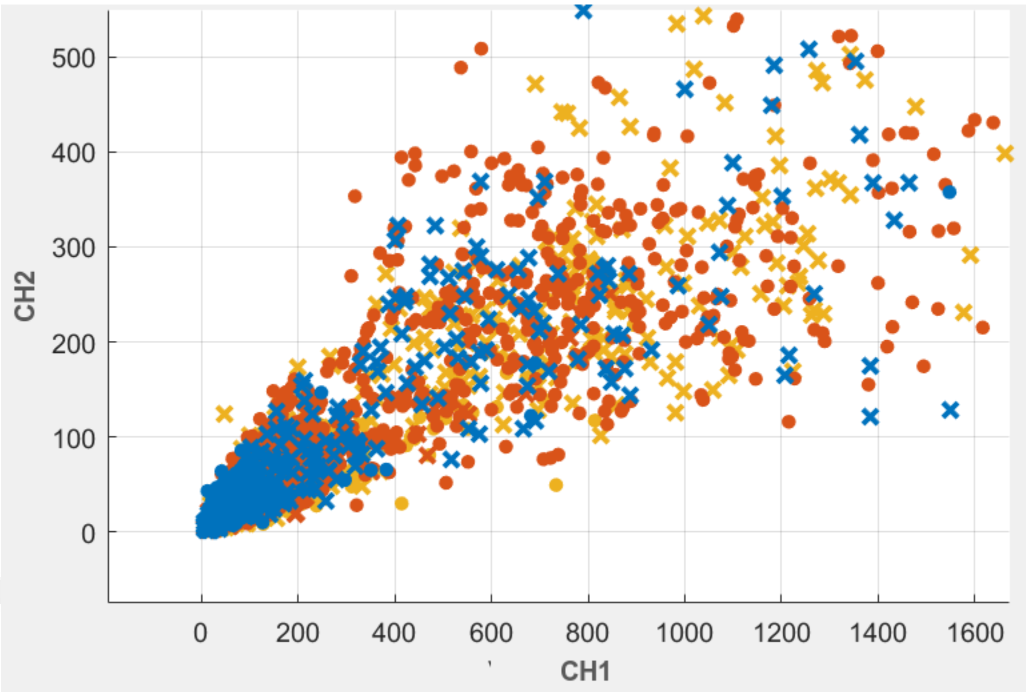

Figure 3.9: SVM Model Predictions of Band Power with Three Classes.

3.1.2.2 Band power accuracy and other measures results

Using the linear feature set, band power, our proposed system was evaluated for its ability to predict lactate enzyme levels in the athlete's body. The pre- and post-exercise measures of lactate enzyme where reported differ widely. They were within the 1-3 millimol/L range for lactate-level-low class, while the post exercise was between 5-8 and above 10-13 millimol/L ranges for the lactate-level-mid class and lactate-level-high classes respectively. When applying this feature set, models had shown a significant score results in terms of accuracy, precision, recall and F1-score.

Application of different models' classification metrics were showing that K-NN over scored other models. With k=5 for the model accuracy cross validation where the data fed to the model was splitter into 5 folds, with band power feature accuracy was reported in its highest values by using the K-NN, followed by the DT whereas LD and SVM came lastly showing the most least performance score. Accuracy was above 99% for the high-level class, as well as for the mid and low-level classes. Secondly, the DT model followed K-NN with results above 98% for the low-level class, whereas scores reported lower for both mid and high class with 97%. The LDA had achieved moderate results with more than 95% with high and mid class, but achieved lower with 93% for the low class, while the SVM showed the lowest score results and were ranging from 78% for mid class, 81% for high class, but scored better for the low class with 88%. When using different value of k-fold validator, k=10, the situation has not changed widely, and the K-NN model still over scored other models. Accuracy reported again above 99% for all the three classes by K-NN model. DT model came in the second place with scores around 98% for the high and mid-level classes, whereas scored better with the low-level class by above 99%. In the third place we reported the LDA model by scoring around 95% for high and mid classes, whereas scored lower with the low-level class by achieving around 93%. The SVM model came last in the list by achieving 89% with the low class, 81% with mid class and 83% with high class.

Other performance measures can be seen by noticing the detailed scores regarding them included within Tables 3.4 and 3.5 for 5-fold and 10-fold cross validation respectively.

Table 3.4: Band Power Results with 5-fold Cross Validation.

Classifier	K-fold	Classes	Accuracy%	Recall%	F1-Score%	Precision%
K-NN	5	Low	99.93	100	100	100
		Mid	99.80	100	100	100
		High	99.77	100	100	100
SVM		Low	88.39	84	82	80
		Mid	78.98	61	76	99
		High	81.10	99	62	45
LDA		Low	93.53	89	90	92
		Mid	95.54	96	93	91
		High	95.72	93	94	94
DT		Low	98.92	98	98	99
		Mid	97.73	98	96	95
		High	97.66	95	97	98

Table 3.5: Band Power Results with 10-Fold Cross Validation.

Classifier	K-fold	Classes	Accuracy%	Recall%	F1-Score%	Precision%
K-NN	10	Low	99.93	100	100	100
		Mid	99.83	100	100	100
		High	99.82	100	100	100
SVM		Low	89.05	80	84	90
		Mid	81.03	68	74	81
		High	82.99	87	70	59
LDA		Low	92.97	87	90	92
		Mid	94.95	96	92	88
		High	95.33	92	93	94
DT		Low	99.23	99	99	99
		Mid	98.15	97	97	97
		High	97.99	97	97	97

In the same time, we had found and reported that the ROC curves shown in figures 3.10 and 3.11, reflects the superiority of the K-NN over other classification models. This confirms the previous finding that it can discriminate between classes better than others in terms of many classification measures, which means it could be applied to other test unseen (test) data and classify between positive and negative data samples by better rates.

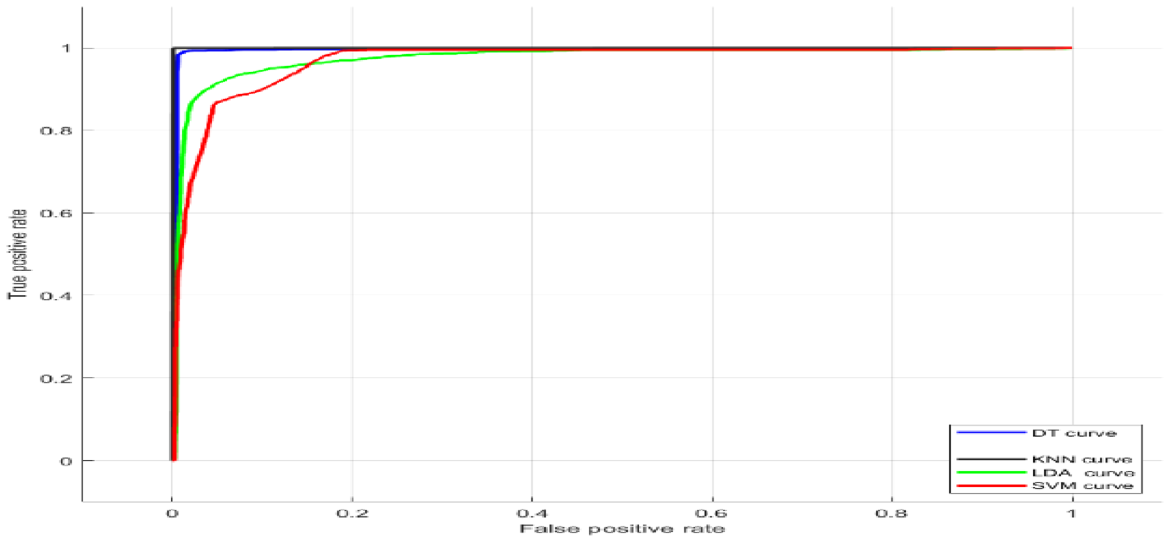

Figure 3.10: ROC of BP for Different Types of Classifiers with 5-Folds.

Each point on the ROC curve reflects a model prediction result representing each of one of the confusion matrix components belonging to that model. Here, we can see that the ROC curve belonging to K-NN model has the best result, since it is located near from the best point (0,1) on the graph, which reflects the fact that we have result with perfect sensitivity, so we have no false negatives, and we have the perfect specificity, so we have no false positives. On the contrary, the curve belonging to the SVM model gives the worst result, since it is located far from the best and deviates toward the depth between 0.2 and 0.8 points.

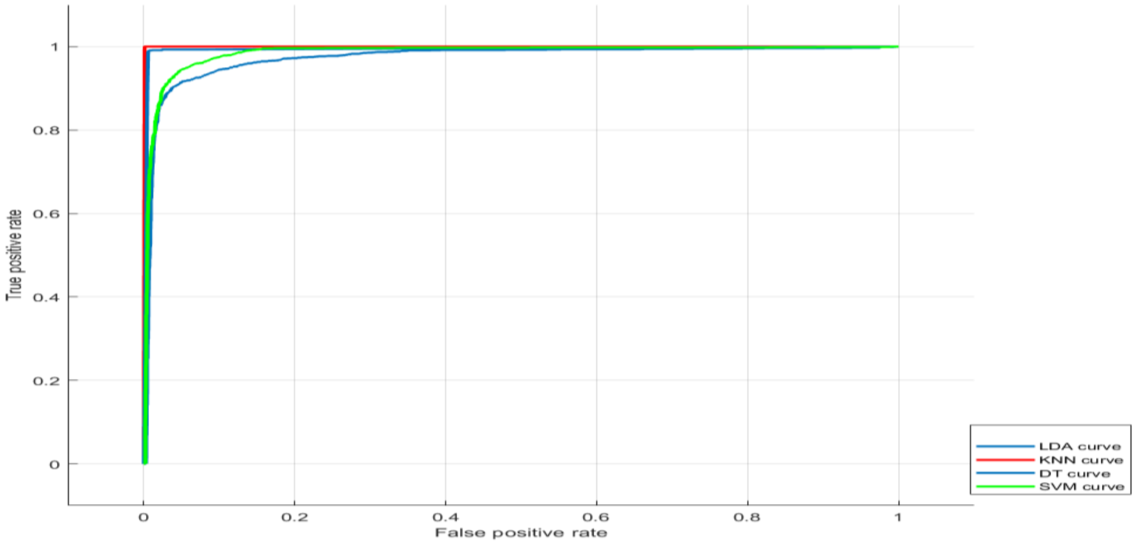

Figure 3.11: ROC of BP for Different Types of Classifiers with 10-Folds.

3.1.2.3 Sample entropy sample features visualization

In our study and for the first time we will be using a new feature of the time series EEG signals namely Sample Entropy (SaEn). As a measure of uncertainty, SaEn will be used will try to find the probability that a certain part of the signal recording could be found to repeat itself (matches) along the entire data series. Firstly, we will provide a visual representation to that feature set extracted from the EEG recording collected from the subjects before and after doing exercise. As shown in figure 3.12, it is clear that this feature (SaEn) had given us a very useful and a good distinguishing criterion that even with only our vision, we can successfully noticeable classification task. By looking at the plot, we easily find that the first feature class is spread within the left most part of the graph and distinguished by the red coloured dots, while the second class with the blue dotes is majorly distributed in the central region of the graph, whereas the third class denoted by the yellow coloured dotes is general distributed in the right most side of the graph with a noticeable amount of samples spread through other regions in the presented graph.

This finding contrasted with that of the previous feature set, Band Power (BP), as it did not show the same ability to visually get the ease of the classification or discrimination task expected outcomes, even though that BP feature gave us high results in different term of performance measure metrics.

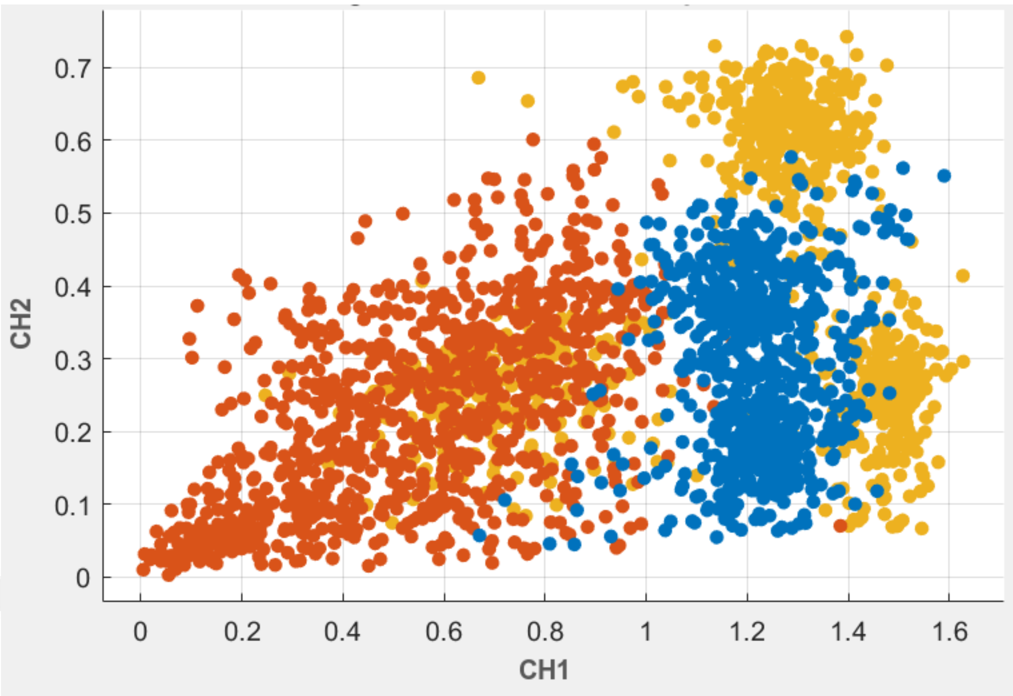

Figure 3.12: Sample of Three Classes Sample Entropy Feature Set.

As with the previous studied and reported feature set, the same classification models were applied again, LDA, SVM, DT and K-NN. These models classification results firstly are plotted to see visually differences between their classes discrimination abilities as shown in figures 3.13, 3.14, 3.15, and 3.16 respectively.

The successfully applied train against test data split ratio is applied also (80/20), as it gave us the promising results from the trained model, which was satisfied by the test portion of the data sets, then finally applying the model score validation technique, K-fold validation, with the two values, 5 and 10.

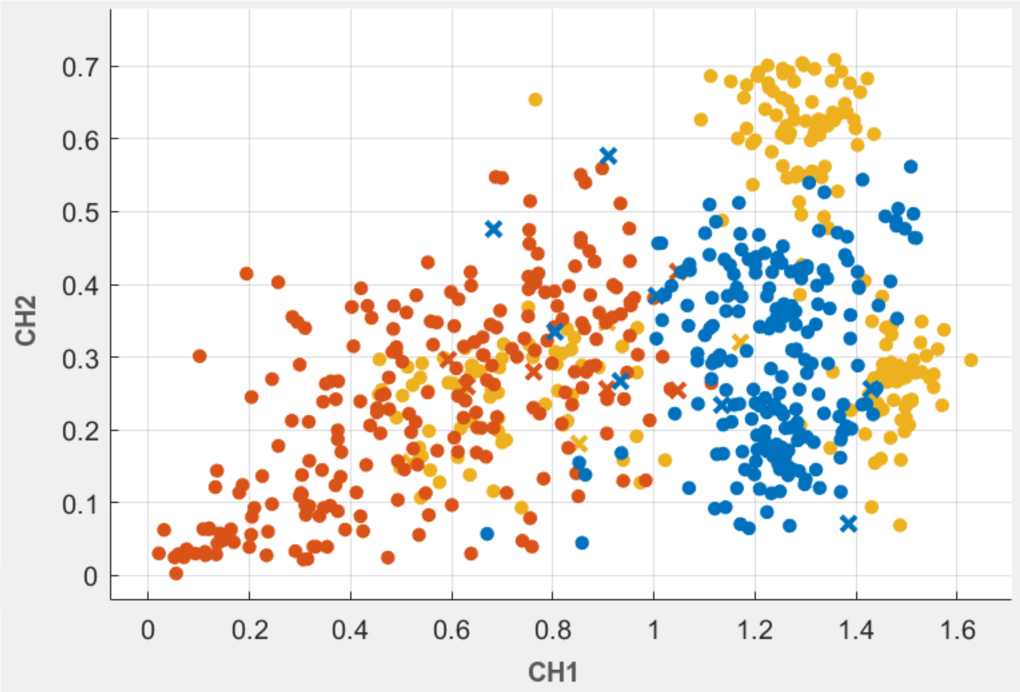

Figure 3.13: Three Classes Sample Entropy DT Model Predictions.

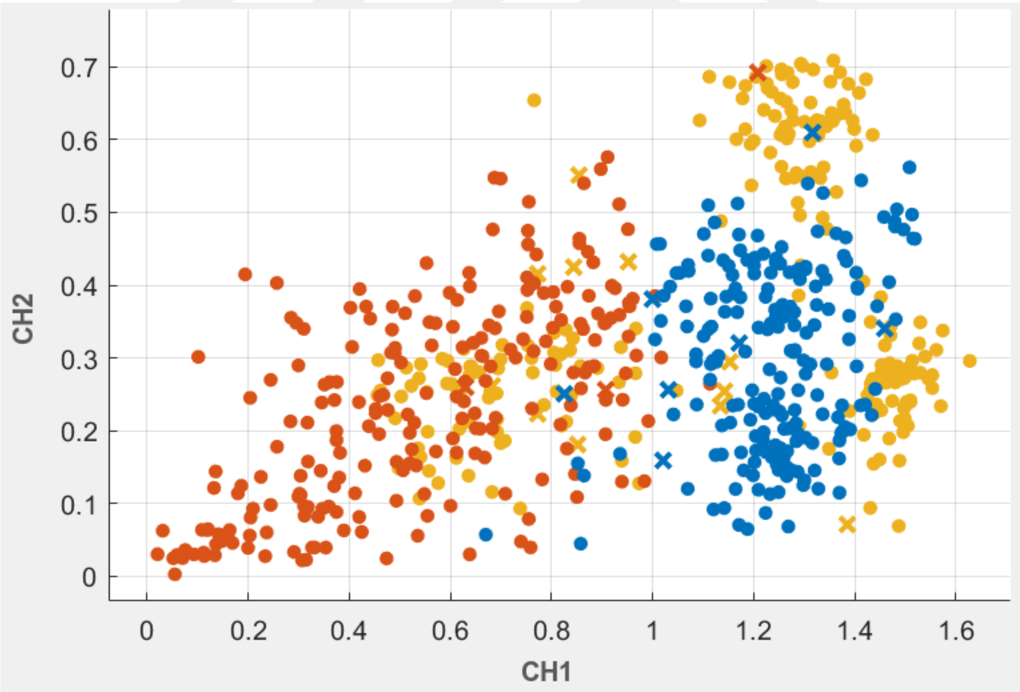

Figure 3.14: Three Classes Sample Entropy LDA Model Predictions.

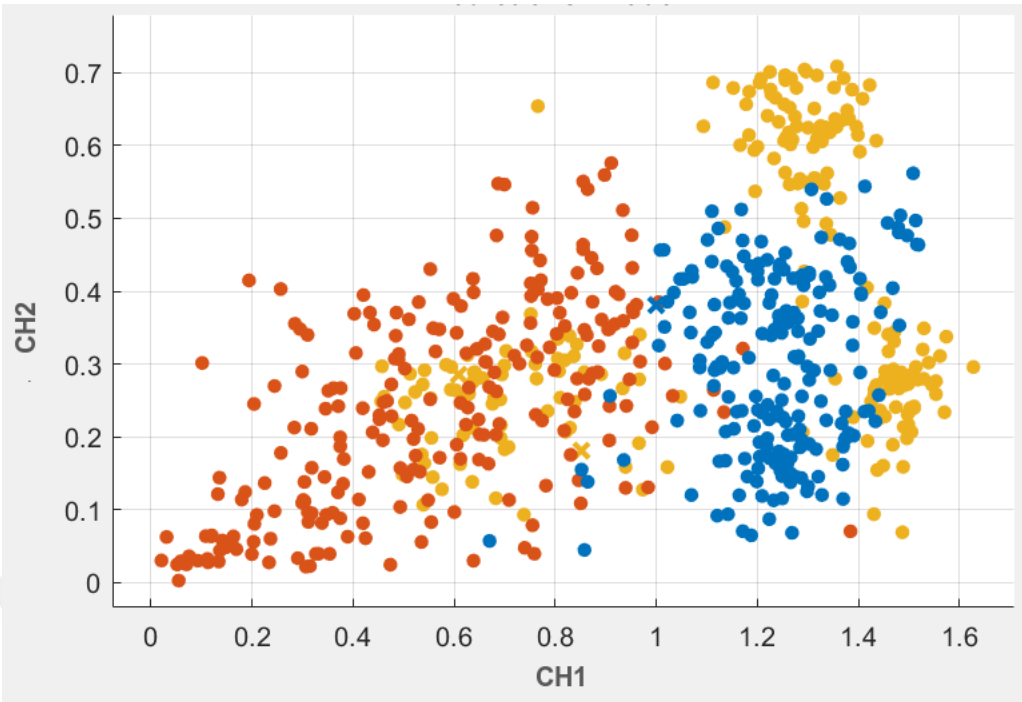

Figure 3.15: Three Classes Sample Entropy K-NN Model Predictions.

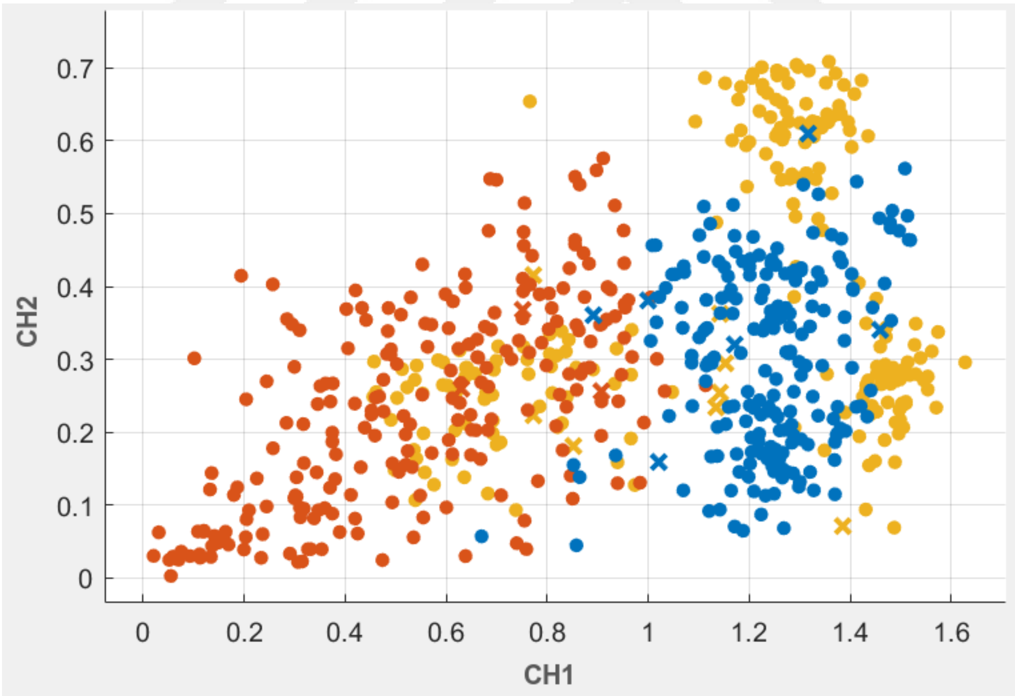

Figure 3.16: Three Classes Sample Entropy SVM Model Predictions.

3.1.2.4 Sample entropy accuracy and other measures results

By using the nonlinear proximity measure SaEn as a feature, we have tested our PTCS system for the advanced three classes prediction task with same goal, if or not it can differentiate between different human blood lactate levels which reflect how does subjects physical tiredness level affected and can be monitored by the means of analysing EEG signals, before and after doing certain kind of exercises. As can be noticed by Table 3.6, with a 5-fold validation, that both K-NN and SVM classifiers had achieved the best scores regarding the performer model accuracy by more than 99% successful recognition rate for all the three classes. The DT classifier on the other hand came next by achieving moderate scores above 98% with both low and high lactate classes, whereas with mid class it scored less by 97%. The LDA came last by scoring barely above 97% with both mid and high classes but scored better with the low class by barely above 98%. Regarding other performance metrics, the case still the same as both K-NN and SVM are taking the lead by scoring better than other models, with one exception at the Recall value for DT model with a score equal to the leading models by achieving 99%.

Table 3.6: Sample Entropy Feature Results with 5-Fold Cross Validation.

Classifier	K-fold	Classes	Accuracy%	Recall%	F1-Score%	Precision%
K-NN	5	Low	99.47	99	99	99
		Mid	99.32	99	99	99
		High	99.32	99	99	99
SVM		Low	99.58	99	99	99
		Mid	99.39	99	99	99
		High	99.35	99	99	99
LDA		Low	98.22	97	97	97
		Mid	97.76	97	97	97
		High	97.42	95	96	96
DT		Low	98.33	97	97	98

Table 3.6: Sample Entropy Feature Results With 5-Fold Cross Validation. "tables continued"

		Mid	97.46	96	97	97
		High	98.82	99	98	97

Table 3.7: Sample Entropy Feature Results with 10-Fold Cross Validation.

Classifier	K-fold	Classes	Accuracy%	Recall%	F1-Score%	Precision%
K-NN	10	Low	99.39	99	99	99
		Mid	99.24	99	99	99
		High	99.54	100	100	100
SVM		Low	99.62	100	99	99
		Mid	99.51	99	99	99
		High	99.43	99	99	99
LDA		Low	98.29	98	97	97
		Mid	97.76	97	97	97
		High	97.34	96	96	96
DT		Low	96.17	93	94	95
		Mid	92.94	91	90	89
		High	95.18	92	92	92

With 10-fold cross validation, there are a few changes noticed by observing scores in Table 3.7 above. In terms of accuracy results, the SVM classifier came first with 99.62%, followed by the K-NN with 99.54%, whereas LDA and DT came next by achieving 97.74% and 96.17% respectively.

The ROC measures related to the proximity measure feature set are shown in figure 3.17 for 5-fold cross validation, and in figure 3.18 for 10-fold cross validation. With 5-folds, and as it was noticed that all classification models had achieved scores with a narrow margin between each, that results have been reflected also and seen as a very close ROC curves to each other and were near from the best point (0,1), which denotes that it was a good measure to observe visually that those classifiers have a very good prediction ability with sensitivity close to perfect state, as well as close to perfect specificity.

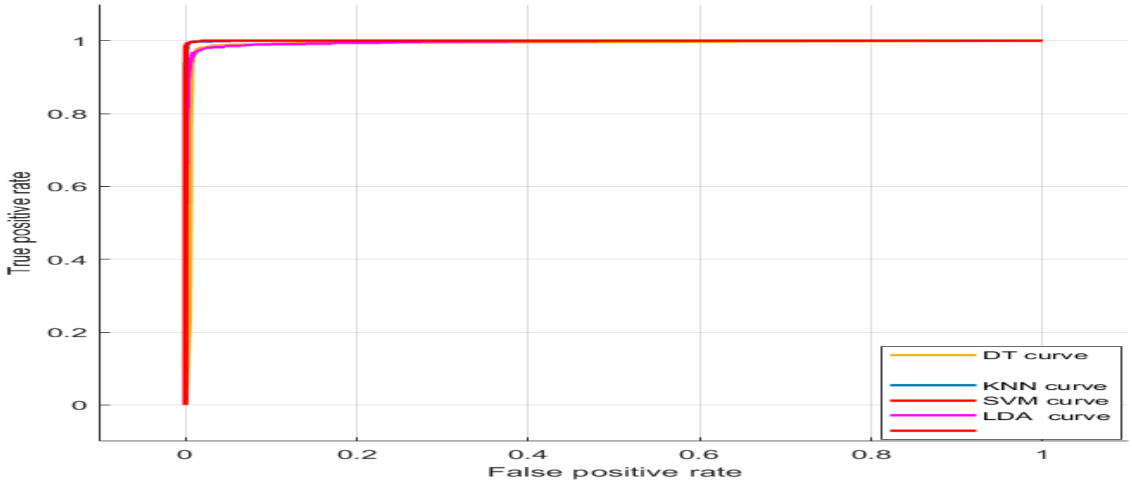

Figure 3.17: ROC for Different Types of Classifiers with 5-Folds Cross Validation.

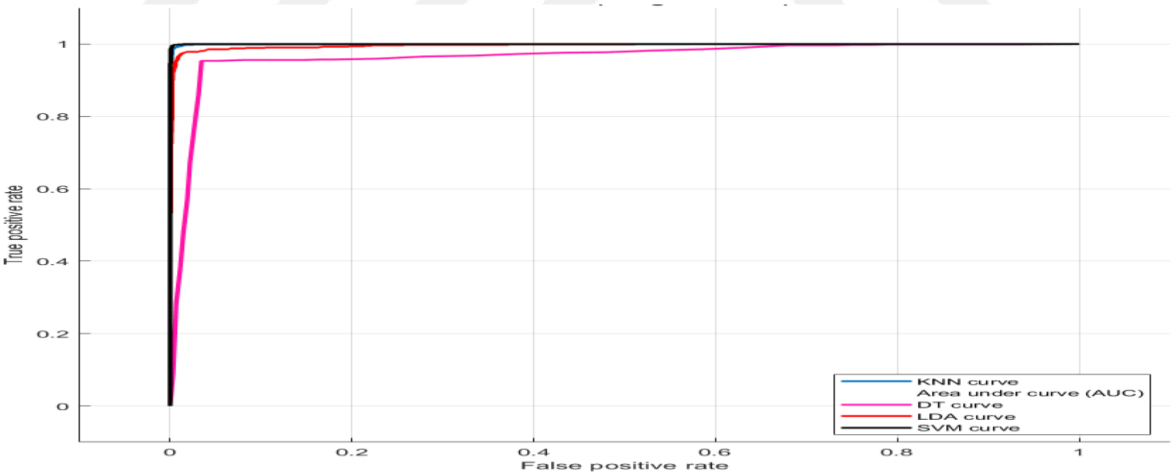

Figure 3.18: ROC for Different Types of Classifiers with 10-Folds Cross Validation.

While in figure 3.17, we can see that there is a slightly variation between ROC area scores belonging to different classification models means that some classification models over sored others. At the same time, we reported that the ROC curves shown in figure 3.18, reflects the obvious dominance of both SVM and K-NN over others denoted by the black and blue curves respectively, whereas the LDA's curve came next by the red colour, and last in the graph had come the DT curve by the pink that means it was worst by the sensitivity to specificity ratio and recognized the positive attribute from negative ones with the lowest rate. This shows us that the modulation of the K-fold cross validation can affect the results of many performances classification measures previous finding that it can discriminate between classes better than others in terms of many classification measures.

According to these observations, the above results listed in [77], show that our proposed PTCS system, and with different feature selection algorithms, had obviously proven its ability to overcome the shortcomings encountered with other methodologies exist in the literature and provided us with a good tool that we can rely on in the goal of classification between various states of the human physical tiredness levels, low, moderate, or high non-invasively using resting state EEG recordings.

3.2 DISCUSSION

The goal set for our study was based on the concept of providing a framework methodologically utilizes the prediction of different human tiredness levels. These levels reflect various situations at which, the lactate enzyme concentration increases in the human blood depending on the tiredness status the body reaches. We refer to these specific levels as lactate level high, representing the very-tired class, or lactate level mid representing the moderate-tired class, or finally the lactate level low representing the not-tired class. The proposed PTCS system tries to answer the following question, can we predict those situations (levels) only by using the EEG measurements collected from the head non-invasively?

The subjects brain signal activations influenced by doing a certain type of aerobic exercise of acute nature was used to prove that goal by our study. Two types of EEG signal features were extracted and fed to the system in the sense of problem classification. In the first part we used only the linear metric BP feature with a two classes prediction task, while three classes of either BP feature or a multivariate complexity SaEn feature was used in the task of the second part. The results gained by the proposed methodology that uses a machine learning technique, have shown that it can accurately, with high performance measures score, to predict lactate enzyme levels when validating them against the measures taken invasively. The proved idea which was set as a goal by the study represents the novelty part that wasn't discussed by another study in literature to the best of our knowledge. Different performance measures like precision, accuracy and others had shown, and among the classification models used, that the K-NN and DT were the winning models compared to SVM and LDA when applying the BP feature, whilst when applying SaEn feature, we found that K-NN with SVM this time had the lead over DT and LDA models as we saw in the results section previously.

In the present study, we had investigated the ability to predict whether the lactate level is low or high in the human body using EEG signals with the use of machine learning algorithms. First, we have used the BP feature, as it was proven to give a good discrimination power for previous studies, due to band power changes of EEG bands derived by performing exercise [78]. In this study, they have collected EEG signals from a group of 25 healthy subjects without any skeletal, muscular, or neurological illness history. The EEG data recording was made by the left cortical area from two electrodes, (C3 and FC3) and the recording process lasted for 45 seconds, whereas in our study, the data used was collected from 16 electrodes for 10 minutes. They have applied a fatigue exercise to the maximum voluntary contraction of the Adductor Pollicis muscle (right one), driven by the motor cortex, in order to study its electrical variations. While recording the EEG signals with a specialized acquisition instrument, they had applied a signal low pass filtering 100 Hz and high pass filtering 1.0 Hz techniques that insure only the desired signal well be collected and reduce the noises. As we have found by our study that the band power of EEG signal had increased as a result of fatigue induced by acute shuttle run exercise, which is compatible with their findings especially for the Alpha and Beta bands. The same hypothesis was found to be studied by [30]. Although there was only an increased tendency of the Alpha band in the frontal sites, but there is not a significant change. Electrical activations of Beta band were found to increase in F3, Fp1, F4 and C4 electrodes only. On the other hand, increase in power for both Alpha and Beta bands was reported by [79]. They have studied changes in Alpha and Beta bands after performing cycle ergometer with increased workload while in progress. A group of 20 men with good health conditions had contributed to the experimental process. They were setting in a comfort manner on the cycle ergometer with eyes open, while initial EEG data acquisition was made twice for 1 minute in each session to record the baseline before activation. The subjects had started the exercise of cycle ergometer with 50Watts with an increase pace, knowing that every 2 minutes the cycling increases by 50Watts until the participant get exhausted. They had collected larger amount of EEG data as they recorded 1 minutes long with 512 Hz sampling rate, but still less than our recordings. Recordings, and for noise and artefact removal aims, have been low and high-pass filtered between 40 Hz and 3 Hz respectively. For the studied bands, Theta, Alpha and Beta, band power was noticed to increase significantly, especially at advanced stages of the exercise where the cortical is activated when exercise passes the 6^{th} minute and subjects starts approaches exhaust state. As the same finding that we deduced, the increase in all bands remained steady near the peak values it reached and did not fall again to the baseline only after the 10^{th} minute, where the body starts to relax again and muscles start returning to the normal oxygen levels, and the lactate enzyme tends to decrease in the blood. When applying machine learning techniques with the use of EEG data for the goal of utilising this methodology in predicting different vital human body signs, they had shown a promising result in the literature. Emotiv device of the low-resolution type was used by a study to give an efficient classification method that can distinguish accurately between variations of face movements using EEG signals [80]. The signals were gathered using 128 Hz rate and data have been filtered within the 0.1 Hz – 32 Hz range to provide signals with minimal noise and artefact from 14 electrodes. The 10 subjects with healthy body state had participated in the experiment. They have used the collected data that represent 4 classes, Clench, Right smirk, Left smirk and no-action by providing them to a K-NN classification method, which had score 96.1%, whereas in our study, the model had achieved 98.4% with 2 classes band power, and above 99% with 3 classes for both band power and sample entropy features.

While we have investigated the changes in band power driven by fatigue state followed a Shuttle run exercise, a study had investigated the same criteria but within doing the exercise [38]. The experiment of maximum free contraction of quadriceps that involves sitting in a calm fashion on a chair with the knee was bending naturally with 90°. The subject was required to extend his/her knee to the maximum until he reaches the fatigue state, meanwhile the EEG signals are being recorded simultaneously by acquisition device with a sampling rate of 128 Hz. They had passed the desired EEG data, after filtering and feature selection processes, to a SVM model for classification purpose. They have achieved 90% score result for their case data, while we have achieved 89% with the BP feature, whereas with the SaEn feature the SVM model had reached the 99% accuracy score.

Table 3.8: Results Comparison with Other Studies.

Study	Year	Electrode no.	Study objective	Applied algorithm	Accuracy %	Recording time	Affected bands
[76]	2004	2	Compute changes of EEG power levels due to maximum voluntary exercise	NA	NA	45 sec	Alpha, Beta
[30]	2007	4	Investigate beta and alpha variations after performing acute exercise	NA	NA	8 min	Beta
[79]	2004	8	Examine changes in EEG spectrum for multiple parts of the cortex during exercise.	NA	NA	1 min	Theta, Alpha, Beta
[80]	2016	14	Predict different facial movements by using EEG activations	K-NN	96.1	NA	NA
[38]	2019	19	Classification of EEG band energy with fatigue level exercise	SVM	90.0	NA	NA
[39]	2022	32	Study effect of exercise on spectral power and signal entropy of EEG signal	ANN and SVM	88.0 and 85.0	15	Delta, Theta, Alpha, Beta
Present study	2022	16	Predict lactate using EEG recordings	K-NN, LDA, DT, SVM	99.0	10 min	Delta, Theta, Alpha, Beta

In the previously mentioned studies researchers had attributed the increase in band power in some bands of EEG signal, especially for Beta one, to the cause of cortical activation elevation, or the driven by doing acute exercise, our because that it is associated with the movement planning and processing in the central and frontal brain areas [12], [81]. For the best of our knowledge, no one of the literature's studies had considered examining changes in the EEG potentials activity derived by acute exercise for the use of predicting human tiredness levels, denoted by lactate enzyme. As though, we proposed our method and barely could compare it with the investigations by studies we found in the literature as shown in Table 3.8 above.

4. CONCLUSION AND FUTURE WORK

4.1 CONCLUSION

The main finding of our present study is developing the PTCS model that predicts different human body tiredness states, not-tired, moderate-tired, or tired denoted by blood lactate enzyme levels affected by brain signal activation after performing a single bout of acute level exercise. This model was tested on a private collected elite athletic EEG dataset of using a variety of classifiers (DT, KNN, LDA, LR, SVM).

The first objective set for this study was to define a model which is presented to the goal of addressing prediction between two classes of BLa concentration in the human body, high or low. These levels were studied by using an EEG data (16 channels) set collected from a group of elite level karate members of national Turkish team (9 subjects) before and after performing exercise. In this part of the research, we applied signal pre-processing methods and cleaned those signals from unwanted artifacts and noises, then we extracted the power spectral densities of each band using FFT technique. Power of the band will act as the classification feature set, before exercise low-class and after exercise high-class. Experimental results of this part show that BP gave us a very good discriminative feature that enabled the proposed model to classify the intended lactate classes with a high-performance measure score, that overcame the performance of the state-of- the-art models.

As the second objective set for this study, we given a model which is presented to the goal of prediction between three classes of BLa concentration rather than two. While in the first objective we extracted and discussed only the BP feature set, here we had discussed and compared between BP and the SaEn as well. The presented model built from a double point of view:

a. Accommodating between different signal pre-processing techniques to clean the raw EEG signals from undesired artefacts and noises.

b. Employing feature extraction methods to extract the best features, complexity, and power spectral of EEG signals that gives the highest degree of differentiation between instances belonging to 3 classes reflecting lactate enzyme levels low, mid, and high.

c. Feeding the resulting feature data sets to various machine learning models and compare between them in terms of performance measure metrics like accuracy and precision.

d. The experimental results demonstrate the robustness of our proposed PTCS model which shows superiority over the state of the arts feature extraction and classification models, before and after performing a single bout of acute exercise.

4.2 FUTURE WORK

Several suggestions can be considered as for a future work project from our study. Here we illustrate different problems as motivations as follows:

a. Use the proposed system scheme for prediction of the human mental tiredness levels by analysing the EEG recordings.

b. Apply the proposed system or a variation of it for the goal of accurate detection of different human hormone levels related to the cognitive or physical exercise.

c. Applying a high-level deep learning techniques to provide a better understanding of the underlying mental activity under a variety of situations for a healthy and sick subject.

d. Employ a feature extraction and selection methods to select the better number of EEG data channels for the dimensionality reduction purposes.

REFERENCES

[1] S. Sanei, & A. Cichocki, *EEG Signal Processing*. 1st ed. Cardiff, UK: Wiley, 2007.

[2] L. W. Ko, Y. Chang, P. L. Wu, H. A. Tzou, S. F. Chen, S. C. Tang, & Y. J. Chen, "Development of a smart helmet for strategical BCI applications," *Sensors*, vol. 19, no. 8, p. 1867, 2019.

[3] T. H. H. Aldhyani and M. R. Joshi, "Integration of time series models with soft clustering to enhance network traffic forecasting," in *2016 Second International Conference on Research in Computational Intelligence and Communication Networks (ICRCICN)*, Kolkata, India, 2016, pp. 212–214.

[4] R. Vigario, J. Sarela, V. Jousmiki, M. Hamalainen, and E. Oja, "Independent component approach to the analysis of EEG and MEG recordings," *IEEE Transactions on Biomedical Engineering*, vol. 47, no. 5, pp. 589–593, 2000.

[5] T. H. H. Aldhyani, A. S. A. Alshebami, and M. Y. Alzahrani, "Soft Computing Model to Predict Chronic Diseases.," *Journal of Information Science and Engineering*, vol. 36, no. 2, pp. 365–376, 2020.

[6] F. Lotte, L. Bougrain, A. Cichocki, M. Clerc, M. Congedo, A. Rakotomamonjy, & F. Yger, "A review of classification algorithms for EEG-based brain-computer interfaces: a 10 year update.," *Journal of Neural Engineering*, vol. 15, no. 3, p. 31005, 2018.

[7] T. B. Weng, G. L. Pierce, W. G. Darling, D. Falk, V. A. Magnotta, and M. W. Voss, "The acute effects of aerobic exercise on the functional connectivity of human brain networks," *Brain Plasticity*, vol. 2, no. 2, pp. 171–190, 2017.

[8] A. S. Rajab, D. E. Crane, L. E. Middleton, A. D. Robertson, M. Hampson, and B. J. MacIntosh, "A single session of exercise increases connectivity in sensorimotor-related brain networks: a resting-state fMRI study in young healthy adults," *Frontiers in Human Neuroscience*, vol. 8, p. 625, 2014.

[9] B. Gutmann, A. Mierau, T. Hülsdünker, C. Hildebrand, A. Przyklenk, W. Hollmann, & H. K. Strüder, “Effects of Physical Exercise on Individual Resting State EEG Alpha Peak Frequency,” *Neural Plasticity*, vol. 2015, p. 717312, 2015.

[10] A. D. Duru, T. H. Balcioğlu, C. E. Özcan Çakir, and D. Göksel Duru, “Acute changes in electrophysiological brain dynamics in elite karate players,” *Iranian Journal of Science and Technology, Transactions of Electrical Engineering*, vol. 44, no. 1, pp. 565–579, 2020.

[11] S. Schneider, C. D. Askew, J. Diehl, A. Mierau, J. Kleinert, T. Abel, & H. K. Strüder, “EEG activity and mood in health orientated runners after different exercise intensities,” *Physiology & Behavior*, vol. 96, no. 4–5, pp. 709–716, 2009.

[12] K. A. Kubitz and A. A. Mott, “EEG power spectral densities during and after cycle ergometer exercise,” *Research Quarterly for Exercise and Sport*, vol. 67, no. 1, pp. 91–96, 1996.

[13] H. Enders, F. Cortese, C. Maurer, J. Baltich, A. B. Protzner, and B. M. Nigg, “Changes in cortical activity measured with EEG during a high-intensity cycling exercise,” *Journal of Neurophysiology*, vol. 115, no. 1, pp. 379–388, 2016.

[14] M. Rahman, W. Karwowski, M. Fafrowicz, and P. A. Hancock, “Neuroergonomics applications of electroencephalography in physical activities: a systematic review,” *Frontiers in Human Neuroscience*, vol. 13, p. 182, 2019.

[15] N. Fujitsuka, T. Yamamoto, T. Ohkuwa, M. Saito, and M. Miyamura, “Peak blood lactate after short periods of maximal treadmill running,” *European Journal of Applied Physiology and Occupational Physiology*, vol. 48, no. 3, pp. 289–296, 1982.

[16] A. Mohamed, O. N. Uçan, O. Bayat, and A. D. Duru, “Classification of resting-state status based on sample entropy and power spectrum of electroencephalography (EEG),” *Applied Bionics and Biomechanics*, vol. 2020, 2020.

[17] A. Craik, Y. He, and J. L. Contreras-Vidal, “Deep learning for electroencephalogram (EEG) classification tasks: a review,” *Journal of Neural Engineering*, vol. 16, no. 3, p. 31001, 2019.

[18] M. N. Anastasiadou, M. Christodoulakis, E. S. Papathanasiou, S. S. Papacostas, and G. D. Mitsis, "Unsupervised detection and removal of muscle artifacts from scalp EEG recordings using canonical correlation analysis, wavelets and random forests," *Clinical Neurophysiology*, vol. 128, no. 9, pp. 1755–1769, 2017.

[19] M. Arabi, M. Dirani, R. Hourani, W. Nasreddine, J. Wazne, S. Atweh, & A. Beydoun, "Frequency and stratification of epileptogenic lesions in elderly with new onset seizures," *Frontiers in Neurology*, vol. 9, p. 995, 2018.

[20] H. Aghajani, M. Garbey, and A. Omurtag, "Measuring mental workload with EEG+ fNIRS," *Frontiers in Human Neuroscience*, vol. 11, p. 359, 2017.

[21] V. Gao, F. Turek, and M. Vitaterna, "Multiple classifier systems for automatic sleep scoring in mice," *Journal of Neuroscience Methods*, vol. 264, pp. 33–39, 2016.

[22] A. Jalilifard, E. B. Pizzolato, and M. K. Islam, "Emotion classification using single-channel scalp-EEG recording," in *2016 38th Annual International Conference of the IEEE Engineering in Medicine and Biology Society (EMBC)*, Orlando, FL, USA, 2016, pp. 845–849.

[23] M. Bentlemsan, E.-T. Zemouri, D. Bouchaffra, B. Yahya-Zoubir, and K. Ferroudji, "Random forest and filter bank common spatial patterns for EEG-based motor imagery classification," in *2014 5th International Conference on Intelligent Systems, Modelling and Simulation*, Langkawi, Malaysia, 2014, pp. 235–238.

[24] J. Hu, "Comparison of different features and classifiers for driver fatigue detection based on a single EEG channel," *Computational and Mathematical Methods in Medicine*, vol. 2017, 2017.

[25] A. Tenev, S. Markovska-Simoska, L. Kocarev, J. Pop-Jordanov, A. Müller, and G. Candrian, "Machine learning approach for classification of ADHD adults," *International Journal of Psychophysiology*, vol. 93, no. 1, pp. 162–166, 2014.

[26] H. Öztoprak, M. Toycan, Y. K. Alp, O. Arikan, E. Doğutepe, and S. Karakaş, "Machine-based classification of ADHD and nonADHD participants using time/frequency features of event-related neuroelectric activity," *Clinical Neurophysiology*, vol. 128, no. 12, pp. 2400–2410, 2017.

[27] A. Arsalan, M. Majid, S. M. Anwar, and U. Bagci, "Classification of perceived human stress using physiological signals," in *2019 41st Annual International Conference of the IEEE Engineering in Medicine and Biology Society (EMBC)*, Berlin, Germany, 2019, pp. 1247–1250.

[28] M. Saeidi, W. Karwowski, F. V. Farahani, K. Fiok, R. Taiar, P. A. Hancock, & A. Al-Juaid, "Neural decoding of EEG signals with machine learning: a systematic review," *Brain Sciences*, vol. 11, no. 11, p. 1525, 2021.

[29] A. Ghosh, F. Dal Maso, M. Roig, G. D. Mitsis, and M.-H. Boudrias, "Unfolding the effects of acute cardiovascular exercise on neural correlates of motor learning using convolutional neural networks," *Frontiers in Neuroscience*, vol. 13, p. 1215, 2019.

[30] H. Moraes, C. Ferreira, A. Deslandes, M. Cagy, F. Pompeu, P. Ribeiro, & R. Piedade, "Beta and alpha electroencephalographic activity changes after acute exercise," *Arquivos de Neuro-psiquiatria*, vol. 65, no. 3-A, pp. 637–641, 2007.

[31] D. M. Devilbiss, J. L. Etnoyer-Slaski, E. Dunn, C. R. Dussourd, M. V. Kothare, S. J. Martino, & A. J. Simon, "Effects of exercise on EEG activity and standard tools used to assess concussion," *Journal of Healthcare Engineering*, vol. 2019, 2019.

[32] S. Nishifuji, "EEG recovery enhanced by acute aerobic exercise after performing mental task with listening to unpleasant sound," in *2011 Annual International Conference of the IEEE Engineering in Medicine and Biology Society*, Boston, MA, USA, 2011, pp. 3837–3840.

[33] D. Büchel, T. Lehmann, Ø. Sandbakk, and J. Baumeister, "EEG-derived brain graphs are reliable measures for exploring exercise-induced changes in brain networks," *Scientific Reports*, vol. 11, no. 1, pp. 1–13, 2021.

[34] D. Büchel, Ø. Sandbakk, and J. Baumeister, “Exploring intensity-dependent modulations in EEG resting-state network efficiency induced by exercise,” *European Journal of Applied Physiology*, vol. 121, no. 9, pp. 2423–2435, 2021.

[35] J. B. Crabbe and R. K. Dishman, “Brain electrocortical activity during and after exercise: a quantitative synthesis,” *Psychophysiology*, vol. 41, no. 4, pp. 563–574, 2004.

[36] C.-J. Huang, C.-W. Huang, Y.-J. Tsai, C.-L. Tsai, Y.-K. Chang, and T.-M. Hung, “A preliminary examination of aerobic exercise effects on resting EEG in children with ADHD,” *Journal of Attention Disorders*, vol. 21, no. 11, pp. 898–903, 2017.

[37] S. Schneider, V. Brümmer, T. Abel, C. D. Askew, and H. K. Strüder, “Changes in brain cortical activity measured by EEG are related to individual exercise preferences,” *Physiology & Behavior*, vol. 98, no. 4, pp. 447–452, 2009.

[38] Z. Yang and H. Ren, “Feature extraction and simulation of EEG signals during exercise-induced fatigue,” *IEEE Access*, vol. 7, pp. 46389–46398, 2019.

[39] O. R. Contreras-Jordán, R. Sánchez-Reolid, Á. Infantes-Paniagua, A. Fernández-Caballero, and F. T. González-Fernández, “Physical Exercise Effects on University Students’ Attention: An EEG Analysis Approach,” *Electronics*, vol. 11, no. 5, p. 770, 2022.

[40] Y. Xiong, J. Gao, Y. Yang, X. Yu, and W. Huang, “Classifying driving fatigue based on combined entropy measure using EEG signals,” *International Journal of Control and Automation*, vol. 9, no. 3, pp. 329–338, 2016.

[41] K. Jawabri, "Physiology, Cerebral Cortex Functions," *Stat Pearls [internet]*, 2022.

[42] E. Kropf, S. K. Syan, L. Minuzzi, and B. N. Frey, “From anatomy to function: the role of the somatosensory cortex in emotional regulation,” *Brazilian Journal of Psychiatry*, vol. 41, pp. 261–269, 2018.

[43] A. Kafkas and E. M. Migo, “Familiarity and recollection in the medial temporal lobe,” *Journal of Neuroscience*, vol. 29, no. 8, pp. 2309–2311, 2009.

[44] M. Arvaneh, C. Guan, K. K. Ang, and C. Quek, “Optimizing the channel selection and classification accuracy in EEG-based BCI,” *IEEE Transactions on Biomedical Engineering*, vol. 58, no. 6, pp. 1865–1873, 2011.

[45] G. A. Light, L. E. Williams, F. Minow, J. Sprock, A. Rissling, R. Sharp, & D. L. Braff, “Electroencephalography (EEG) and event-related potentials (ERPs) with human participants,” *Current Protocols in Neuroscience*, vol. 52, no. 1, pp. 6–25, 2010.

[46] R. D. Pascual-Marqui, “Standardized low-resolution brain electromagnetic tomography (sLORETA): technical details,” *Methods and Findings in Experimental and Clinical Pharmacology*, vol. 24, no. Suppl D, pp. 5–12, 2002.

[47] G. Vrbancic and V. Podgorelec, “Automatic classification of motor impairment neural disorders from EEG signals using deep convolutional neural networks,” *Elektronika ir Elektrotechnika*, vol. 24, no. 4, pp. 3–7, 2018.

[48] J. J. Newson and T. C. Thiagarajan, “EEG frequency bands in psychiatric disorders: a review of resting state studies,” *Frontiers in Human Neuroscience*, vol. 12, p. 521, 2019.

[49] M. Abo-Zahhad, S. M. Ahmed, and S. N. Abbas, “A new EEG acquisition protocol for biometric identification using eye blinking signals,” *International Journal of Intelligent Systems and Applications*, vol. 7, no. 6, p. 48, 2015.

[50] J. F. Cavanagh and M. J. Frank, “Frontal theta as a mechanism for cognitive control,” *Trends in Cognitive Sciences*, vol. 18, no. 8, pp. 414–421, 2014.

[51] A. Visser, D. Büchel, T. Lehmann, and J. Baumeister, “Continuous table tennis is associated with processing in frontal brain areas: an EEG approach,” *Experimental Brain Research*, vol. 240, no. 6, pp. 1–11, 2022.

[52] A. Sofiah and H. Zakaria, “Calculation of Quantitative Parameters of Clinical EEG Signals by Adopting Visual Reading Methods,” in *2018 International Symposium on Electronics and Smart Devices (ISESD)*, Bandung, Indonesia, 2018, pp. 1–7.

[53] C. Lainscsek, M. E. Hernandez, J. Weyhenmeyer, T. J. Sejnowski, and H. Poizner, “Non-linear dynamical analysis of EEG time series distinguishes patients with Parkinson’s disease from healthy individuals,” *Frontiers in Neurology*, vol. 4, p. 200, 2013.

[54] B. J. Roach and D. H. Mathalon, “Event-related EEG time-frequency analysis: an overview of measures and an analysis of early gamma band phase locking in schizophrenia,” *Schizophrenia Bulletin*, vol. 34, no. 5, pp. 907–926, 2008.

[55] S. J. Kiebel, J. M. Kilner, and K. J. Friston, “Hierarchical models for EEG and MEG,” in *Statistical Parametric Mapping: The Analysis of Functional Brain Images*, 1'st ed. London: AP Elsevier Ltd., 2007, ch. 16, pp. 211–222.

[56] G. Wolberg, “Fast Fourier transforms: A review,” Columbia University, New York, NY, Rep. Technical Report CUCS-388-88, 1988.

[57] S. Keshmiri, “Entropy and the brain: An overview,” *Entropy*, vol. 22, no. 9, p. 917, 2020.

[58] J.-R. Huang, S.-Z. Fan, M. F. Abbod, K.-K. Jen, J.-F. Wu, and J.-S. Shieh, “Application of multivariate empirical mode decomposition and sample entropy in EEG signals via artificial neural networks for interpreting depth of anesthesia,” *Entropy*, vol. 15, no. 9, pp. 3325–3339, 2013.

[59] J. M. Yentes, N. Hunt, K. K. Schmid, J. P. Kaipust, D. McGrath, and N. Stergiou, “The appropriate use of approximate entropy and sample entropy with short data sets,” *Annals of Biomedical Engineering*, vol. 41, no. 2, pp. 349–365, 2013.

[60] A. Delgado-Bonal and A. Marshak, “Approximate entropy and sample entropy: A comprehensive tutorial,” *Entropy*, vol. 21, no. 6, p. 541, 2019.

[61] Q. Liu, L. Ma, S.-Z. Fan, M. F. Abbod, and J.-S. Shieh, “Sample entropy analysis for the estimating depth of anaesthesia through human EEG signal at different levels of unconsciousness during surgeries,” *PeerJ*, vol. 6, p. e4817, 2018.

[62] G. J. Jiang, S. Z. Fan, M. F. Abbod, H. H. Huang, J. Y. Lan, F. F. Tsai, & J. S. Shieh, "Sample entropy analysis of EEG signals via artificial neural networks to model patients' consciousness level based on anesthesiologists experience," *BioMed Research International*, vol. 2015, 2015.

[63] L. A. Leger, D. Mercier, C. Gadoury, and J. Lambert, "The multistage 20 metre shuttle run test for aerobic fitness," *Journal of Sports Sciences*, vol. 6, no. 2, pp. 93–101, 1988.

[64] R. J. Robertson, "Exercise testing and prescription using RPE as a criterion variable," vol. 32, no. 2, pp. 177–188, 2001.

[65] G. A. V Borg, "Psychophysical bases of perceived exertion.," *Medicine & Science in Sports & Exercise*, vol. 14, no. 5, pp. 377-381, 1982.

[66] N. Gebodh, Z. Esmaeilpour, D. Adair, K. Chelette, J. Dmochowski, A. J. Woods, & M. Bikson, "Inherent physiological artifacts in EEG during tDCS," *NeuroImage*, vol. 185, pp. 408–424, 2019.

[67] N. S. Bastos, B. P. Marques, D. F. Adamatti, and C. Z. Billa, "Analyzing EEG signals using decision trees: A study of modulation of amplitude," *Computational Intelligence and Neuroscience*, vol. 2020, 2020.

[68] S. Sperandei, "Understanding logistic regression analysis," *Biochemia medica*, vol. 24, no. 1, pp. 12–18, 2014.

[69] M. Szumilas, "Explaining odds ratios," *Journal of the Canadian Academy of Child and Adolescent Psychiatry*, vol. 19, no. 3, pp. 227-229, 2010.

[70] P. Eusebi, "Diagnostic accuracy measures," *Cerebrovascular Diseases*, vol. 36, no. 4, pp. 267–272, 2013.

[71] S. A. Shaban, O. N. Ucan, and A. D. Duru, "Classification of lactate level using resting-state EEG measurements," *Applied Bionics and Biomechanics*, vol. 2021, 2021.

[72] N. Brodu, F. Lotte, and A. Lécuyer, “Comparative study of band-power extraction techniques for motor imagery classification,” in *2011 IEEE Symposium on Computational Intelligence, Cognitive Algorithms, Mind, and Brain (CCMB)*, Paris, France, 2011, pp. 1-6.

[73] R. Jenke, A. Peer, and M. Buss, “Feature extraction and selection for emotion recognition from EEG,” *IEEE Transactions on Affective Computing*, vol. 5, no. 3, pp. 327–339, 2014.

[74] J. Atkinson and D. Campos, “Improving BCI-based emotion recognition by combining EEG feature selection and kernel classifiers,” *Expert Systems with Applications*, vol. 47, pp. 35–41, 2016.

[75] M. Adeva-Andany, M. López-Ojén, R. Funcasta-Calderón, E. Ameneiros-Rodríguez, C. Donapetry-García, M. Vila-Altesor, & J. Rodríguez-Seijas, “Comprehensive review on lactate metabolism in human health,” *Mitochondrion*, vol. 17, pp. 76–100, 2014.

[76] C. J. Valvona, H. L. Fillmore, P. B. Nunn, and G. J. Pilkington, “The regulation and function of lactate dehydrogenase a: therapeutic potential in brain tumor,” *Brain Pathology*, vol. 26, no. 1, pp. 3–17, 2016.

[77] S. A. Shaban, S. Al-jumaili, O. N. Ucan, & A. D. Duru, “Evaluation of machine learning algorithms in the prediction of tiredness level using the complexity and band power measurements of brain activity,” *Traitement du Signal*, submitted 3 Nov. 2022.

[78] A. A. Abdul-latif, I. Cosic, D. K. Kumar, B. Polus, and C. Da Costa, “Power changes of EEG signals associated with muscle fatigue: the root mean square analysis of EEG bands,” in *Proceedings of the 2004 Intelligent Sensors, Sensor Networks and Information Processing Conference*, Melbourne, Australia, 2004, pp. 531–534.

[79] S. P. Bailey, E. E. Hall, S. E. Folger, and P. C. Miller, “Changes in EEG during graded exercise on a recumbent cycle ergometer,” *Journal of Sports Science & Medicine*, vol. 7, no. 4, p. 505, 2008.

[80] U. I. Awan, U. H. Rajput, G. Syed, R. Iqbal, I. Sabat, and M. Mansoor, “Effective classification of EEG signals using K-nearest neighbor algorithm,” in *2016 International Conference on Frontiers of Information Technology (FIT)*, Islamabad, Pakistan, 2016, pp. 120–124.

[81] L. M. F. Doyle, K. Yarrow, and P. Brown, “Lateralization of event-related beta desynchronization in the EEG during pre-cued reaction time tasks,” *Clinical Neurophysiology*, vol. 116, no. 8, pp. 1879–1888, 2005.